Sirt7 protects against vascular calcification via modulation of reactive oxygen species and senescence of vascular smooth muscle cells

Sirt7 protects against vascular calcification via modulation of reactive oxygen species and senescence of vascular smooth muscle cells

Hongjiao Yu[1,2#], Yuchen Xie[3#], Lan Lan[4#], Siyu Ma[2], Simon Wing Fai Mok[5], Io Nam Wong[5], Yueheng Wang[3], Guoli Zhong[3], Liang Yuan[3], Huan Zhao[3], Xiao Hu[6], Vicky E Macrae[7], Shengping He[8*], Guojun Chen[6*], Dongxing Zhu[3*]

1. Department of Hepatobiliary and Pancreatic Surgery, The Second Affiliated Hospital, Guangzhou Medical University, Guangzhou, 510260, China
2. GMU-GIBH Joint School of Life Sciences, The Guangdong-Hong Kong-Macao Joint Laboratory for Cell Fate Regulation and Diseases, Guangzhou Medical University.
3. Guangzhou Institute of Cardiovascular Disease, Guangdong Key Laboratory of Vascular Diseases, State Key Laboratory of Respiratory Disease, The Second Affiliated Hospital, School of Basic Medical Sciences, Guangzhou Medical University, Guangzhou, Guangdong, 510260, China.
4. Department of Anesthesiology, The First Affiliated Hospital of Guangzhou Medical University, Guangzhou, China.
5. Faculty of Medicine, Macau University of Science and Technology, Taipa, Macau, China.
6. Department of Cardiology, Guangdong Provincial Key Laboratory of Cardiac Function and Microcirculation, State Key Laboratory of Organ Failure Research, Nanfang Hospital, Southern Medical University, Guangzhou, China
7. Functional Genetics and Development, The Royal (Dick) School of Veterinary Studies and The Roslin Institute, University of Edinburgh, Midlothian, UK.
8. Department of Cardiovascular Surgery, Nanfang Hospital, Southern Medical University, 1838 North Guangzhou Avenue, Guangzhou, Guangdong 510515, China.

H. Yu, Y. Xie and L. Lan should be considered joint first authors.

Running title: The protective role of *Sirt7* in vascular calcification

***Address for correspondence:** Dongxing Zhu, PhD, Email: dongxing.zhu@gzhmu.edu.cn, Tel: +86.020.37103613, Guangzhou Institute of Cardiovascular Disease, Guangdong Key Laboratory of Vascular Diseases, State Key Laboratory of Respiratory Disease, The Second Affiliated Hospital, Guangzhou Medical University, Guangzhou, Guangdong, 510260, China; Shengping He, MD, Email: hsp@smu.edu.cn, Tel: +86.020.62786468, Department of Cardiovascular Surgery, Nanfang Hospital, Southern Medical University, 1838 North Guangzhou Avenue, Guangzhou, Guangdong 510515, China; Guojun Chen, MD, PhD, Email: chenguojun@i.smu.edu.cn, Tel: +86.020.62786284, Department of Cardiology, State Key Laboratory of Organ Failure Research, Nanfang Hospital, Southern Medical University, Guangzhou, China.
[1]

Abstract

Vascular calcification is frequently seen in patients with chronic kidney disease (CKD), and significantly increases cardiovascular mortality and morbidity. *Sirt7*, a NAD^+-dependent histone deacetylases, plays a crucial role in cardiovascular disease. However, the role of *Sirt7* in vascular calcification remains largely unknown. Using *in vitro* and *in vivo* models of vascular calcification, this study showed that *Sirt7* expression was significantly reduced in calcified arteries from mice administered with high dose of vitamin D_3 (vD_3). We found that knockdown or inhibition of *Sirt7* promoted vascular smooth muscle cell (VSMC), aortic ring and vascular calcification in mice, whereas overexpression of *Sirt7* had opposite effects. Intriguingly, this protective effect of *Sirt7* on vascular calcification is dependent on its deacetylase activity. Unexpectedly, *Sirt7* did not alter the osteogenic transition of VSMCs. However, our RNA-seq and subsequent studies demonstrated that knockdown of *Sirt7* in VSMCs resulted in increased intracellular reactive oxygen species (ROS) accumulation, and induced an Nrf-2 mediated oxidative stress response. Treatment with the ROS inhibitor N-acetylcysteine (NAC) significantly attenuated the inhibitory effect of *Sirt7* on VSMC calcification. Furthermore, we found that knockdown of *Sirt7* delayed cell cycle progression and accelerated

[1]**Abbreviations**: Chronic kidney disease, CKD; vitamin D_3, vD_3; vascular smooth muscle cell, VSMC; reactive oxygen species, ROS; N-acetylcysteine, NAC; phosphate, Pi; runt-related transcription factor 2, RUNX2; bone morphogenetic protein-2, BMP2; alkaline phosphatase, ALPL; tumor necrosis factor alpha, TNF-α; transforming growth factor-β, TGF-β; blood urea nitrogen, BUN; creatinine, CREA; uric acid, UA; nicotinamide, NAM.

cellular senescence of VSMCs. Taken together, our results indicate that *Sirt7* regulates vascular calcification at least in part through modulation of ROS and cellular senescence of VSMCs. *Sirt7* may be a potential therapeutic target for vascular calcification.

Keywords: Vascular calcification, *Sirt7*, Reactive oxygen species, cellular senescence

1. Introduction

Vascular calcification is a pathological process characterized by abnormal deposition of calcium and phosphate (Pi) crystals in the vascular wall [1]. It is commonly seen, and significantly increases the risk of cardiovascular complications in patients with chronic kidney disease (CKD) [2]. Despite its severe clinical consequences, there is currently no effective treatment to prevent or reverse vascular calcification. A better understanding of the molecular mechanisms regulating vascular calcification may therefore lead to the development of novel therapeutic strategy for this disease, and ultimately reduce cardiovascular mortality and morbidity in CKD patients.

Considerable evidence demonstrates that vascular calcification is an active, and highly regulated pathological process that show many similarities to that of bone formation. Vascular smooth muscle cells (VSMCs), the major cell type in the vascular wall, have a critical role in vascular calcification [3]. CKD patients commonly develop hyperphosphatemia, which is a strong inducer of vascular calcification [4]. Congruently, we and others have previously reported that high Pi treatment promotes VSMC osteogenic transition and calcification *in vitro* [5-7]. This phenotypic transition of VSMCs is characterized by an increase in the expression of osteogenic markers such as runt-related transcription factor 2 (RUNX2), bone morphogenetic protein-2 (BMP2), and alkaline phosphatase (ALPL) [8].

Cellular senescence, a state of irreversible cell-cycle arrest of mitotic cells, has also been implicated in the pathogenesis of vascular calcification [9]. Senescent VSMCs are characterized by telomere shortening, increased oxidative DNA damage or impaired DNA repair, and are associated with increased expression of BMP2 as well as pro-inflammatory cytokines such as interleukin-1β (IL-1β), interleukin-6 (IL-6) and tumor necrosis factor alpha (TNF-α) [10], which are key regulators of vascular calcification. Intriguingly, accumulated senescent vascular cells have been found during high Pi-induced VSMC calcification *in vitro*, and adenine-induced rat vascular calcification *in vivo* [11]. Consistent with these results, replicative senescence of VSMCs has been shown to promote osteogenic transition and vascular calcification [12]. Intriguingly, Pi binders such as lanthanum carbonate and calcium carbonate can prevent high Pi-induced VSMC premature senescence and vascular calcification [13].

Oxidative stress resulting from overproduction of reactive oxygen species (ROS) and/or by reduced expression of antioxidant enzymes is a major stimulus for vascular cell senescence [14]. Oxidative stress and excessive production of ROS have been reported to promote VSMC osteogenic transition and calcification [15]. Local excessive ROS formation generated by a novel laser-based method induces vascular degeneration and calcification, supporting a direct role of ROS in vascular calcification [16]. Consistent with these results, elevated ROS production and expression of key regulators of ROS (e.g. NADPH oxidase) are seen in calcified arteries in CKD rats [17]. Oxidative stress and ROS-induced cellular senescence may therefore be attractive therapeutic targets for the treatment of vascular calcification.

The Sirtuin (*Sirt*) family was originally found in yeast as Silent Information Regulator 2, *Sir2* [18]. To date, seven homologs of *Sir2* that have been identified in mammals (*Sirt1*-*Sirt7*). Sirtuins are conserved nicotinamide adenine dinucleotide (NAD^+)-dependent histone deacetylases that regulate a broad range of biological processes such as metabolism, cell survival, longevity and stress resistance [19]. *Sirt7* is the most recently identified mammalian Sirtuin, and it is localized predominantly in the nucleoli and ubiquitously expressed by several tissues in the body including the liver, spleen, and heart [20]. Previous studies have reported that *Sirt7* expression is increased in human breast cancer and hepatocellular carcinoma, and promotes the invasion of cancer cells through H3K18 deacetylation-mediated inhibition of tumor suppressor genes [21-23]. Recent studies have also demonstrated that *Sirt7* plays a key role in the development of cardiovascular disorders. *Sirt7* promotes myocardial tissue repair through regulation of transforming growth factor-β (TGF-β) signaling pathway [24]. Furthermore, *Sirt7* attenuates stress-induced cardiac hypertrophy

and prevents cardiomyocyte apoptosis and inflammatory cardiomyopathy in mice [25-26]. A previous study has reported that *Sirt7* inhibits VSMC proliferation and migration though the Wnt/β-Catenin signaling pathway [27], suggesting an important role for *Sirt7* in regulation of vascular homeostasis and disease. However, whether *Sirt7* directly contributes to the development of vascular calcification remains unclear.

In the present study, we have demonstrated that *Sirt7* protects against vascular calcification, and have explored the underlying mechanisms using a combination of *in vitro* and *in vivo* models of vascular calcification.

2. Materials and Methods

2.1. Animal experiments

All animal experiments were approved by the Institutional Animal Care Committee at Guangzhou Medical University (Ref No: GY2023-169), and performed in accordance with the National Institutes of Health Guide for the Care and Use of Laboratory Animals. Only male mice were used in the present study to exclude the possible influence of the female sex hormone estrogen on vascular calcification [28]. Six-week-old male C57BL/6 J mice were purchased from Guangdong Medical Laboratory Animal Centre, and maintained under standard laboratory conditions with a 12 hr light /12 hr dark cycle and free access to water and food. Mice were randomly divided into three groups (n=5): namely vehicle group, vD_3 group and vD_3+97491 group. Vascular calcification was induced by the administration of a high dose of vitamin D_3 (vD_3) as previously reported by our laboratory [7]. In brief, mice were subcutaneously injected with a dose of vD_3 ($5*10^5$ IU kg−1 per day) (Sigma, PHR1237) or vehicle control for 3 consecutive days, and sacrificed 7 days after the first injection to evaluate vascular calcification by alizarin red staining (Sigma, A5533) and calcium quantitative assay (Sigma, MAK022). The *Sirt7* inhibitor 97491 (MCE, HY-135899) at a concentration of $0.5mg/kg^{-1}$ per day was simultaneously administered by intraperitoneal injection to mice with vD_3 for the first 3 days, and the inhibitor alone at the same dose for the next 4 days until the end of the experiments.

2.2. Plasma biochemical analysis

Blood samples were collected from the right ventricle of mice from vehicle group, vD_3 group and vD_3+97491 group, and plasma was isolated by centrifugation at 3000 g for 5 min at 4°C. Calcium content in the plasma was measured using a colorimetric assay (Sigma, MAK022-1KT) according to the manufacturer's instructions. Plasma levels of Pi and blood urea nitrogen (BUN), creatinine (CREA) and uric acid (UA) were measured using an automatic biochemical analyzer (Rayto, Chemray 800, Shenzhen, China).

2.3. Aortic ring culture

Aortas were carefully isolated from six-week-old male C57BL/6 J mice. After removal of the surrounding adipose tissue, the aortas were cut into 2-3 mm rings, and cultured in growth medium containing α-MEM medium (Gibco, 12571063) with 10% FBS (Gibco, 16000-044), 100 U/mL of penicillin (HyClone, SH40003.01), and 100 mg/ml of streptomycin (Hyclone, SV30010) in 12-well plates in a 37 ℃ incubator with 5% CO_2. To induce calcification, the aortic rings were treated 5 mM Pi in the presence or absence of the Sirtuin inhibitor nicotinamide (NAM) (sigma, N0636) at the indicated concentrations for 7 days. The medium was changed every 3 days.

2.4. Murine VSMC culture and in vitro calcification

The mouse VSMCs were isolated from 12 six-week-old male C57BL/6 J mice and cultured with growth medium as we previously described [29]. To induce VSMC *in vitro* calcification, the cells were treated with 3 mM Pi for up to 14 days. Pi was prepared as a combination of NaH_2PO_4/Na_2HPO_4 with a ratio of 1:3, pH=7.4. The cells were maintained in 95% air/5%CO_2, and the media was changed every third/fourth day. For certain experiments, cells were cultured with calcifying medium and treated with the Sirtuin inhibitor NAM or the reactive oxygen species (ROS) inhibitor N-acetylcysteine (NAC) (Sigma, A0737) at the indicated duration and concentrations.

2.5. Determination of VSMC and aorta calcification

Calcium deposition in murine VSMCs and aortas was determined by alizarin red staining and calcium colorimetric assay as previously reported by our laboratory [29]. For VSMCs, the cells were washed twice with cold PBS, fixed with 4% paraformaldehyde (PFA) for 10 min, stained with 2% alizarin red (pH 4.2) for 10 min at room temperature, and photographed. The cells were also decalcified with 0.6 M HCl at 4°C

overnight. Free calcium in the supernatants was determined using a calcium colorimetric assay (Sigma, MAK022-1KT) according to the manufacturer's instructions. Cells were washed with PBS twice and harvested in lysis buffer (1 mM NaOH/0.1% SDS) for protein extraction. The total protein concentration was determined with bicinchoninic acid (BCA) protein assay kit (Thermo Fisher, 23235). Calcium content was normalized to total cell protein and expressed as μg/mg protein. For aortas, the blood vessels were fixed in 95% ethanol for 24 hrs, stained with 0.0016% alizarin red in 1% potassium hydroxide for 30 hrs, then washed twice with 0.5% potassium hydroxide and photographed with an inverted microscope. The aortic tissues were subsequently de-calcified in 0.6M HCL overnight, and the calcium content were determined by a commercial calcium kit (Sigma, MAK022-1KT) with normalization to the dry weight of the aortas.

2.6. RT-qPCR

Total RNA was extracted from mouse VSMCs or aortas using TaKaRa MiniBEST Universal RNA Extraction Kit (Takara, 9767), and 1μg of total RNA was reverse transcribed using PrimeScript™ RT Master Mix (Takara, RR036A) according to the manufacturer's instructions. RT-qPCR was conducted with SYBR Premix Ex Taq II (Takara, RR820A) in the QuantStudio 5 real-time system (Life technologies). Each PCR was run in triplicate. All gene expression data were calculated using the $2^{-\Delta\Delta CT}$ method and normalized against β-actin. The control values were expressed as 1 to indicate a precise fold change value for each gene of interest. The primer sequences for target genes are summarized in **Supplementary Table S1**.

2.7. Western blotting

VSMCs or aortas were harvested with RIPA lysis buffer (Beyotime Biotechnology, P0013B) containing 1 mM protease inhibitor phenylmethylsulfonyl fluoride (PMSF) (Beyotime Biotechnology, ST505). 10μg of protein lysates were separated on SDS-Polyacrylamide gels and transferred to PVDF membranes. The membranes were incubated overnight at 4 °C with primary antibodies. Subsequently, the membranes were incubated with HRP-conjugated anti-mouse (1:4000, Cell Signaling Technology, 7076S) or anti-rabbit (1:4000, Cell Signaling Technology, 7074S) secondary antibodies for 1 hr at room temperature. The immune complexes were visualized by chemiluminescence Lumi-Light Western Blotting Substrate (Millipore, WBKLS0500). Semi-quantitative assessment of band intensity was performed by ImageJ software (National Institutes of Health). Details of antibodies used in this study are provided in **Supplementary Table S2.**

2.8. siRNA-mediated knockdown of Sirt7

Mouse VSMCs were seeded at the density of $1.0x10^5$ cells/well in 6-well plates, and siRNAs targeting *Sirt7* (si*Sirt7*) or Scrambled siRNAs (siScramble) at a final concentration of 20 nM were transfected using Lipofectamine RNAiMAX (Invitrogen, 13778) according to the manufacturer's instructions. All siRNAs were purchased from Guangzhou RiboBio Co., Ltd, China. The knockdown efficiency of *Sirt7* was validated by RT-qPCR and Western blotting. For VSMC *in vitro* calcification and senescence experiments, cells were re-transfected every 7 days during the experiments to maintain the optimal knockdown efficiency. The sequences of scrambled siRNAs are not disclosed by this company. The siRNA sequences targeting *Sirt7* are provided in **Supplementary Table S3.**

2.9. Adenovirus-mediated overexpression of Sirt7

Recombinant adenoviruses expressing flag-tagged *Sirt7* (Ad-*Sirt7*), flag-tagged *Sirt7*^{H188Y} (a loss-of-function mutant) and adenoviruses containing empty plasmids (Ad-null) that served as negative controls were constructed and purchased from Hanheng Bioscience Incorporation, Shanghai, China. VSMCs were seeded at the density of $1.0x10^5$ cells/well in 6-well plates, and infected with Ad-null, Ad-*Sirt7* or Ad-*Sirt7*^{H188Y} for 48 hrs at multiplicities of infection (MOI) of 100. The overexpression efficiency of *Sirt7* was validated by RT-qPCR and western blotting. For *in vitro* calcification and senescence studies, cells were re-infected every 7 days during the experiments.

2.10. RNA-sequencing

Mouse VSMCs were seeded at a density of 1.0×10^5 cells/well in 6-well plates, and transfected with 20 nM siScrambled or si*Sirt7* for 48 hrs. The cell samples were then sent to KangChen Biotech (Shanghai, People's Republic of China) for RNA sequencing. In brief, total RNA was extracted using Trizol (Invitrogen) according to the manufacturer's protocol. The concentration of total RNA was detected using a NanoDrop ND-1000 spectrophotometer (Thermo Scientific), and the integrity was examined by denaturing agarose gel electrophoresis. A total quantity of 1~2 μg total RNA was purified using oligo (dT) conjugated magnetic beads. RNA-seq libraries were constructed using KAPA Stranded RNA-Seq Library Prep Kit (Illumina), and

monitored using an Agilent Bioanalyzer 2100. RNA sequencing was performed on an Illumina HiSeq 4000 by KangChen Biotech. The RNA-seq data reported in this paper has been deposited in NCBI Gene Omnibus (http://www.ncbi.nlm.nih.gov/geo/) with the accession number of GEO: GSE247550. Raw data are publicly available after Dec 01, 2023.

2.11. Immunofluorescence staining

Mouse VSMCs were seeded on glass coverslips and transfected with 20 nM siScramble or si*Sirt7* for 48 hrs. At the end of the experiments, VSMCs were fixed with 4% PFA, permeabilized with 0.3% triton x-100 (Beyotime Biotechnology, P0013B), and incubated overnight at 4°C with anti-NRF2 (1:200, Abcam, ab137550). After washing three times with PBS, cells were incubated with Alexa Fluor®488 anti-rabbit antibodies (1:1000, Invitrogen, A-11008) at 37 °C for 1 hr in dark. Glass coverslips were then stained with DAPI and the fluorescence signal was detected under Leica DMRB fluorescence microscope (Leica SP8). Negative controls were carried out simultaneously by incubating with equivalent concentrations of normal rabbit IgG (Cell Signaling Technology, 2729s) instead of primary antibody.

2.12. Intracellular ROS staining

VSMCs were seeded at the density of $1.0*10^5$ cells/well in 6-well plates. After confluency, cells were transfected with siScramble or si*Sirt7* at a final concentration of 20 nM, and treated with growth medium and calcifying medium containing 3 mM Pi for 48 hrs. Intracellular ROS levels were detected using the cell-permeable reagent 2',7'-dichlorofluorescein diacetate (DCFHDA/H2DCFDA, ab113851, Abcam) according to the manufacturer's instructions. After the staining, the fluorescence signal was detected under Leica DMRB fluorescence microscope (Leica SP8), and semi-quantified using the ImageJ software.

2.13. Cell cycle assessment

VSMCs were seeded at a density of $3*10^5$ cells in 60-mm culture plates, and transfected with 20 nM siScramble or siSrit7 for 48 hrs in growth medium or calcifying medium. To examine the cell cycle, cells were starved with serum-free medium for 24 hrs, then stimulated with 10% FBS for another 24 hrs. The cells were trypsinized, fixed in 70% ethanol at 4 °C overnight, washed twice with ice-cold PBS and incubated with RNase and propidium iodide. The cell-cycle phase was detected by flow cytometry using a BD FACStar flow cytometer and ModiFit software.

2.14. Senescence-Associated-β Galactosidase Staining

SA-β-Gal staining was performed using a commercially available kit (Beyotime Biotechnology, C0602) according to the manufacturer's instructions. Briefly, mouse VSMCs were transfected with siScramble or si*Sirt7* as described above in the growth medium or calcifying medium for 7 days. At the end of the experiments, mouse VSMCs were fixed with 4% PFA for 10 min at room temperature, washed with PBS for 3 times, and incubated with the staining solution (containing X-gal) at 37 °C (without CO2) for 5 hrs. Images were taken using a microscope and the SA-βG-positive cells was quantified using ImageJ software.

2.15. Statistical analysis

The experimental data in this study are expressed as mean ±SD. Statistical analysis was performed using GraphPad Prism 6 (La Jolla, CA) software. After confirming a normal distribution using the Shapiro-Wilk test, data were analyzed using unpaired Student's t-test for comparison of two groups, or one-way ANOVA followed by Tukey's multiple comparisons test for comparison of multiple groups. P value of <0.05 were considered to be statistically significant.

3. Results

3.1. Sirt7 expression is decreased during vascular calcification

To gain insight into the role of *Sirt7* in vascular calcification, we initially detected its expression in calcified arteries from mice with overloaded vD_3. Alizarin red staining and calcium quantitative assay showed a significant increase in calcium deposition in arteries from mice with overloaded vD_3 **(Figure 1A-C)**. Consistent with previous studies [7], we observed a significant increase in mRNA expression of osteogenic genes including *Runx2*, *Alpl* and *Opn* in calcified mouse arteries compared to controls **(Figure 1D)**. Additionally, we compared the expression of the Sirtuin family (*Sirt1*-*Sirt7*), and found that mRNA expression of *Sirt5*, *Sirt6* and *Sirt7* were significantly down-regulated in calcified mouse arteries compared to controls **(Figure 1D)**. However, mRNA expression of *Sirt1*-*Sirt4* remains unchanged in this mouse model of vascular calcification **(Figure 1D)**. These results are consistent with a recent study showing that *Sirt6* was

down-regulated and had a protective role in vascular calcification [30-31]. *Sirt7* was selected for further investigation in this study as its roles in vascular calcification remains unknown. Our western blotting results further confirmed that *Sirt7* protein expression was significantly reduced in calcified mouse arteries **(Figure 1E)**. These results suggest that *Sirt7* may have an important role in vascular calcification.

3.2. Sirt7 attenuates vascular calcification in vitro and in vivo

We next investigated the functional role of *Sirt7* in vascular calcification. Our results showed that 10 mM Nicotinamide, a pan inhibitor of Sirtuin family, significantly increased high Pi-induced VSMC and aortic ring calcification *in vitro* (**Supplementary Figure S1A-D).** To further confirm the specific effects of *Sirt7* on vascular calcification, siRNA-mediated knockdown of *Sirt7* in VSMCs was performed. RT-qPCR and western blotting results showed that transfection of si*Sirt7* significantly attenuated its mRNA and protein expression in VSMCs after 48 hrs (**Supplementary Figure S2A&C**), but did not alter mRNA expression of other Sirtuin family members including *Sirt1-Sirt6* (**Supplementary Figure S2B)**. Consistent with our previous results, we found that knockdown of *Sirt7* significantly promoted high Pi-induced VSMC *in vitro* calcification, as determined by alizarin red staining and calcium quantitative assay **(Figure 2A&B)**. We also overexpressed *Sirt7* expression in VSMCs using the adenovirus system, and the overexpression efficiency was validated by RT-qPCR and western blotting (**Supplementary Figure S3A-C**)**.** Conversely, adenovirus-mediated overexpression of *Sirt7* attenuated high Pi-induced VSMC *in vitro* calcification, as determined by alizarin red staining and calcium quantitative assay **(Figure 2C&D)**. Intriguingly, this inhibitory effect of *Sirt7* on VSMC calcification was significantly attenuated by a catalytically inactive mutant $Sirt7^{H188Y}$ [32] **(Figure 2C&D)**. 97491 has been recently identified as a specific *Sirt7* inhibitor, which reduces its histodeacetylase activity [33]. We found that the *Sirt7* specific inhibitor 97491 promoted vD_3-induced mouse vascular calcification *in vivo* **(Figure 2E&F)**. However, 97491 treatment did not alter vD_3-induced increase in serum levels of calcium, blood urea nitrogen (BUN), creatinine (CREA) and uric acid (UA) in these mice (**Supplementary Table S4)**. These results suggest that *Sirt7* inhibits vascular calcification depending on its histodeacetylase activity.

3.3. Sirt7 does not regulate the osteogenic transition of VSMCs

To understand the underlying mechanisms through which *Sirt7* regulates vascular calcification, we initially investigated whether *Sirt7* altered the osteogenic transition of VSMCs, a key process during vascular calcification. Unexpectedly, knockdown of *Sirt7* did not significantly change the mRNA and protein expression of osteogenic genes including *Runx2* and *Bmp2* in VSMCs (**Supplementary Figure S4A-C).** In addition, the contractile markers including α-SMA, and SM22α remained unchanged in VSMCs with silencing of Sirt7 (**Supplementary Figure S4C).** Consistently, neither overexpression of *Sirt7* nor its catalytically inactive mutant $Sirt7^{H188Y}$ significantly altered *Runx2* and *Bmp2* expression in VSMCs (**Supplementary Figure S4D-F).** These results suggest that the inhibitory effects of *Sirt7* on vascular calcification is not mediated by the osteogenic transition of VSMCs.

3.4. Knockdown of Sirt7 induces Nrf2-mediated oxidative stress response in VSMCs

To gain the mechanistic insight into the role of *Sirt7* in vascular calcification, we performed RNA sequencing (RNA-Seq) based transcriptomic profiling in VSMCs with silencing of *Sirt7*. Our RNA-Seq results showed that 229 genes were significantly up-regulated, and 312 genes were significantly down-regulated in VSMCs with depleted *Sirt7* **(Figure 3A&B)**. The top 11 up-regulated genes in VSMCs with depleted *Sirt7* are listed including *Gsta1*, *Hmox1*, *Gsta2*, *Gsta3* and *Nqo1* **(Figure 3C)**. Our RT-qPCR confirmed that these genes including *Gsta1*, *Hmox1*, *Gsta2*, *Gsta3* and *Nqo1* were significantly up-regulated in VSMCs with silencing of *Sirt7* **(Figure 3D)**. The top 9 down-regulated genes including *Rgs4*, *Ccnd1* and *Tmem170b* were also validated by RT-qPCR **(Figure 3D)**. A strong correlation between the fold change of the RNA-Seq and RT-qPCR results was seen **(Figure 3E)**. Ingenuity Pathway Analysis (IPA) revealed that the most significantly affected pathways were cell cycle and Nrf2-mediated oxidative stress response in VSMCs with silencing of *Sirt7* **(Figure 3F)**. Of note, Nrf2 is a key transcription factor that senses oxidative stress to initiate the antioxidant response by directly activating the expression of several antioxidative enzymes such as *Gsta1*, *Hmox1*, *Gsta2*, *Gsta3* and *Nqo1*[34]. In accordance with these results, we found that knockdown of *Sirt7* significantly increased nuclear translocation of Nrf2, as revealed by immunofluorescence staining **(Figure 3G)**. Antioxidative genes *Gsta1*, *Hmox1*, *Gsta2*, *Gsta3* and *Nqo1* were also significantly up-regulated in VSMCs with depleted expression of *Sirt7*, as revealed by RNA-seq and RT-qPCR **(Figure 3C&D)**.

SQSTM1/p62 and Keap1 are key regulators of Nrf2 activation [35]. Our RNA-seq results showed that

silencing of *Sirt7* in VSMCs significantly increased *Sqstm1/p62* mRNA expression but did not alter *Keap1* mRNA expression **(Figure 3H)**. Comparable increased expression of SQSTM1/p62 protein expression was also seen in VSMCs with depleted Sirt7 **(Figure 3I)**. It is well known that SQSTM1/p62 protein expression is selectively degraded by autophagy, we therefore examined whether *Sirt7* regulated autophagy in VSMCs [36]. Our RNA-seq results demonstrated that silencing of *Sirt7* in VSMCs did not alter the key regulators of autophagy including *Atg2a*, *Atg2b*, *Atg3*, *Atg4a*, *Atg5*, *Atg7* and *Becn1***(Supplementary Figure S5A)**. Consistently, western blotting and immunofluorescence staining showed that *Sirt7* knockdown did not alter the expression of autophagy maker LC3 expression **(Supplementary Figure S5B&C).** In addition, treatment with bafilomycin-A1, an inhibitor of autophagic flux, did not prevent *Sirt7* knockdown-induced increased protein expression of SQSTM1/p62 in VSMCs **(Supplementary Figure S5D).** Taken together, these results suggest that silencing of *Sirt7* may transcriptionally increase SQSTM1/p62 expression, leading to activation of Nrf2-mediated oxidative stress response, which is independent of autophagy.

3.5. Knockdown of Sirt7 accelerates high Pi-induced VSMC calcification through increased intracellular ROS production

Having shown that knockdown of *Sirt7* induces a Nrf2-mediated oxidative stress response, we next examined whether *Sirt7* regulates ROS accumulation in VSMCs. As expected, we found that silencing of *Sirt7* significantly increased intracellular ROS in VSMCs at day 2, as revealed by DCFHDA staining **(Figure 4A&B)**. ROS is mainly produced by xanthine oxidoreductase (XDH), mitochondrial respiratory enzymes and nicotinamide adenine dinucleotide phosphate (NADPH) oxidase in vascular cells [37]. We found that knockdown of *Sirt7* in VSMCs did not alter mitochondrial ROS production, as revealed by MitoSox staining **(Figure 4C)**. In addition, our RNA-seq results showed that knockdown of *Sirt7* did not change NADPH oxidase *Nox4* mRNA expression yet significantly increased *Xdh* mRNA expression in VSMCs **(Figure 4D)**. Increased XDH protein expression was also seen in VSMCs with depleted *Sirt7* expression in both the presence and absence of high Pi **(Figure 4E)**. Intriguingly, the ROS inhibitor NAC significantly attenuated *Sirt7* knockdown-induced increase in VSMC calcification *in vitro* **(Figure 4F)**. These findings suggest that *Sirt7* may regulate vascular calcification through altered intracellular ROS production.

3.6. Knockdown of Sirt7 delays cell cycle progression and increases cellular senescence

Our RNA-seq and IPA pathway analysis also revealed that knockdown of *Sirt7* resulted in the enrichment of gene signatures involved in cell cycle **(Figure 3F).** In accordance with these data, we performed a FACs based cell cycle analysis, and showed that silencing of *Sirt7* significantly increased the percentage of VSMCs in G1-phase **(Figure 5A&B)**. In addition, the cell cycle regulators including p-RB and Cyclin D1 were significantly down-regulated in VSMCs with depletion of *Sirt7* **(Figure 5C).** These results suggest that knockdown of *Sirt7* delayed cell cycle progression of VSMCs. Cell cycle arrest typically results in cellular senescence. Our initial studies confirmed that cellular senescence was increased during high Pi-induced VSMC *in vitro* calcification **(Supplementary Figure S6A-E)**. Consistent with these results, we found that knockdown of *Sirt7* in VSMCs significantly accelerated cellular senescence, as revealed by SA-β-Gal staining **(Figure 5D&E).** In mammals, cellular senescence is typically induced by the activation of two canonical signaling pathways including p16-pRB pathway (stress response) and the p53-p21 pathway (DNA damage response) [38]. We observed that knockdown of *Sirt7* increased p16 expression but not p21 expression in VSMCs **(Figure 5F).** These results suggest that *Sirt7* may also regulate vascular calcification through modulation of vascular cell senescence.

4. Discussion

In this study, we identified a previously uncharacterized role of *Sirt7* in vascular calcification. We showed that *Sirt7* expression was significantly down-regulated in calcified arteries from mice with overloaded vD_3. We found that both silencing and inhibition of *Sirt7* accelerated high Pi-induced aortic ring and VSMC calcification *in vitro*. In addition, inhibition of *Sirt7* histodeacetylase activity using the compound 97491 promoted vD_3-induced mouse vascular calcification *in vivo*. On the other hand, adenovirus-mediated overexpression of *Sirt7* attenuated high-Pi induced VSMC *in vitro* calcification, whereas this inhibitory effect was significantly attenuated by $Sirt7^{H188Y}$, a catalytically inactive mutant. Mechanistically, we showed that *Sirt7* did not alter the osteogenic transition of VSMCs. Our RNA-seq and the following experiments demonstrated that *Sirt7* regulated vascular calcification at least in part through modulation of ROS production and cellular senescence of VSMCs. These results increase our current understanding of epigenetic regulation of vascular calcification, and suggest that *Sirt7* may be a potential therapeutic target for vascular calcification.

Sirt7, the most recently identified mammalian Sirtuins, has a critical role in the development of cardiovascular disease. *Sirt7* knockout mice show a reduced lifespan and progressive heart hypertrophy and inflammatory cardiomyopathy [25]. *Sirt7* protects from cardiac hypertrophy, and promotes myocardial tissue repair [24,26]. However, the role of *Sirt7* in vascular disease remains unclear. We found that *Sirt7* expression was significantly reduced in calcified arteries from mice with overloaded vD_3. These results are supported by a previous study reporting that *Sirt7* is decreased during VSMC *in vitro* calcification [30]. Using high Pi-induced VSMC *in vitro* calcification model and high dose vD_3-induced mouse vascular calcification model, we for the first time showed that *Sirt7* protected against vascular calcification under CKD conditions. In accordance with our results, a recent study has reported that *Sirt7* attenuates high glucose-induced calcification of myeloid cells, and protects against diabetic vascular disease [39]. This study together with our results indicate an important role of *Sirt7* in vascular calcification under different disease conditions. Importantly, a recent study has reported that *Sirt7* attenuates hypertension-induced renal fibrosis and injury [40]. Hence, we cannot exclude the possibility that *Sirt7* may protect vascular calcification through improve the kidney function during CKD. However, it should be noted that high Pi-induced VSMC calcification and vD_3-induced mouse vascular calcification used in this study may not completely reflect the pathological process of vascular calcification in human CKD patients. Therefore, more clinically relevant animal models of vascular calcification such as adenine or 5/6 nephrectomy-induced CKD rats may be used to further strengthen our observation.

Sirt7 is mainly localized in the nucleus, and function as an NAD^+-dependent histone/protein deacetylase to regulate its target genes [39]. Using a catalytically inactive mutant $Sirt7^{H188Y}$ or a specific chemical inhibitor 97491 that reduces *Sirt7* histodeacetylase activity, we showed that *Sirt7* attenuated vascular calcification *in vitro* and *in vivo* depending on its deacetylase activity. Future studies using unbiased ChIP-sequencing and mass spectrometry may identify the downstream targets of *Sirt7* in vascular cells and their roles in *Sirt7*-mediated inhibition of vascular calcification. Osteogenic transition of VSMCs has an important role in vascular calcification. The role of *Sirt7* in ostengenic transition remains ambiguous. It has reported that knockdown of *Sirt7* enhances osteogenic transition of human bone marrow mesenchymal stem cells partly via activation of the Wnt/β-catenin signaling pathway [41]. However, a contrasting study has shown that *Sirt7* promotes bone formation by deacetylation of osterix [42]. In this study, neither knockdown nor overexpression of *Sirt7* altered the expression of osteogenic genes within VSMCs. Therefore, the function of *Sirt7* in regulation of osteogenic transition may be cell-type specific.

The imbalanced clearance and production of ROS leads to oxidative stress and accumulated ROS, which plays an important role in the development of vascular calcification. It has been reported that increased oxidative stress accelerates vascular calcification, whereas amelioration of oxidative stress attenuates vascular calcification [43, 44]. Our RNA-seq results in *Sirt7*-knockdown VSMCs showed that the up-regulated genes were significantly enriched in Nrf2-mediated oxidative stress response. Subsequent experiments confirmed that Nrf2 translocated into the nucleus in VSMCs with depletion of *Sirt7*, which is possibly due to increased expression p62, a key regulator of Nrf2 activation [35]. Nrf2 is activated in response to oxidative stress. In line with these results, we found that knockdown of *Sirt7* significantly increased ROS accumulation in VSMCs, and inhibition of ROS using NAC significantly attenuated increased VSMC *in vitro* calcification that observed in VSMC with knockdown of *Sirt7*. These results are consistent with a previous study showing that *Sirt7* depletion markedly elevated reactive oxygen species levels in oocytes [45]. In vascular wall, ROS is predominantly generated by the NADPH Oxidase, mitochondria and xanthine oxidase [46]. We found that *Sirt7* knockdown did not alter the expression of the NADPH Oxidase NOX4 and mitochondrial ROS, but significantly increased xanthine oxidase expression. Intriguingly, previous studies have shown that increased xanthine oxidase expression in human atherosclerotic plaque with vascular calcification, and inhibition of xanthine oxidase using allopurinol reduces the development of atherosclerosis in mouse models [47]. Our results suggest that *Sirt7* may regulate vascular calcification at least in part through ROS, and indicate that xanthine oxidase-mediated ROS production may have an important role in vascular calcification. It would be of interest for further studies to investigate whether inhibition of xanthine oxidase exerts protective effects against vascular calcification.

Accumulating evidence supports that cellular senescence of VSMCs is a key pathological characteristic of vascular calcification [48,49]. In accordance with these studies, we found that cellular senescence was significantly increased during high Pi-induced VSMC *in vitro* calcification. Intriguingly, we found that *Sirt7*

depletion significantly attenuated the cell cycle progression, and promoted cellular senescence. In addition, we found that the cellular senescence marker p16 rather than p21 was significantly increased in VSMCs with depletion of *Sirt7*. These results are supported by a recent study reporting a direct transcriptional regulation of p16 by *Sirt7*, thereby leading to cellular senescence in primary human lung fibroblast MRC5 cells [50]. In addition, the accumulated expression of p62 in VSMCs with *Sirt7* depletion seen in this study may also contribute to accelerated cellular senescence, as suggested by a previous study showing that p62 accumulation mediates the induction of senescence in autophagy defective VSMCs [51]. Taken together, these results indicate that cellular senescence may also contribute to the inhibitory role of *Sirt7* in vascular calcification.

A previous study has identified a regulatory loop between *Sirt1* and *Sirt7*, showing that *Sirt7* binds to *Sirt1* to inhibit its activity, thereby regulating the differentiation and maintenance of white adipose tissue [52]. In addition, it has also been found that *Sirt7* and *Sirt1* coordinately enhance osterix activity and promote orthotropic bone formation [43]. Intriguingly, it is well characterized that *Sirt1* inhibits vascular calcification through regulation of DNA damage and RUNX2 signaling under diabetic conditions [53,54]. Therefore, we cannot exclude the possibility that *Sirt7* may also regulate vascular calcification through the crosstalk with *Sirt1*.

In summary, we for the first time demonstrate a protective role of *Sirt7* in vascular calcification. Mechanistically, we show that *Sirt7* attenuates vascular calcification at least in part through regulation of ROS production and cellular senescence of VSMCs. Our study not only broaden our current understanding of epigenetic regulation of vascular calcification, but also sheds light on the possibility to develop novel strategy to treat vascular calcification by targeting *Sirt7*.

Funding

This work was supported by funding from the National Natural Science Foundation of China (82170428, 82370421, 82300485), The 'Yangcheng Scholar' Grant of Guangzhou (202032768), Science and Technology Projects of Guangzhou (202201011067), Guangdong Basic and Applied Basic Research Foundation (2024A1515013008, 2021A1515011663), Project of the State Key Laboratory of Respiratory Disease, Guangzhou Medical University (SKLRD-Z-202223), and Macao Science and Technology Development Fund (0069/2021/AFJ, 0037/2022/ITP).

Data Availability

The data underlying this article will be shared on reasonable request to the corresponding author. The RNA-seq data is available in NCBI Gene Omnibus (http://www.ncbi.nlm.nih.gov/geo/) with the accession number of GEO: GSE247550.

CRediT authorship contribution statement

D. Zhu, **G. Chen** and **S. He** conceived and designed the study. **H. Yu**, **Y. Xie** and **L. Lan** performed the majority of the experiments, and contributed to the acquisition of the data, analysis and interpretation. **S. Ma**, **Y. Wang**, **G. Zhon**g, **L. Yuan**, **H. Zhao**, and **X. Hu** performed the experiments and analyzed the data. **D. Zhu** wrote the manuscript. **I. Wong**, **S. Mok**, **V. Macrae**, **G. Chen**, **S. He**, and **D. Zhu** revised the manuscript. All authors read and accepted the manuscript.

Declaration of competing interest

The authors declare that there is no conflict of interest

Acknowledgements

None

Appendix A. Supplementary data

Supplementary data to this article can be found online.

References

1. Hutcheson JD, Goettsch C. Cardiovascular Calcification Heterogeneity in Chronic Kidney Disease. *Circ Res* 2023;**132**:993-1012.
2. Dube P, DeRiso A, Patel M, Battepati D, Khatib-Shahidi B, Sharma H, Gupta R, Malhotra D, Dworkin L, Haller S, Kennedy D. Vascular Calcification in Chronic Kidney Disease: Diversity in the Vessel

Wall. *Biomedicines* 2021;**9**.
3. Negri AL. Role of prolyl hydroxylase/HIF-1 signaling in vascular calcification. *Clin Kidney J* 2023;**16**:205-209.
4. Hruska KA, Mathew S, Lund R, Qiu P, Pratt R. Hyperphosphatemia of chronic kidney disease. *Kidney Int* 2008;**74**:148-157.
5. Cozzolino M, Ciceri P, Galassi A, Mangano M, Carugo S, Capelli I, Cianciolo G. The Key Role of Phosphate on Vascular Calcification. *Toxins (Basel)* 2019;**11**.
6. Giachelli CM. The emerging role of phosphate in vascular calcification. *Kidney Int* 2009;**75**:890-897.
7. Zhong H, Yu H, Chen J, Mok SWF, Tan X, Zhao B, He S, Lan L, Fu X, Chen G, Zhu D. The short-chain fatty acid butyrate accelerates vascular calcification via regulation of histone deacetylases and NF-kappaB signaling. *Vascul Pharmacol* 2022;**146**:107096.
8. Bundy K, Boone J, Simpson CL. Wnt Signaling in Vascular Calcification. *Front Cardiovasc Med* 2021;**8**:708470.
9. Burton DG, Matsubara H, Ikeda K. Pathophysiology of vascular calcification: Pivotal role of cellular senescence in vascular smooth muscle cells. *Exp Gerontol* 2010;**45**:819-824.
10. Voelkl J, Lang F, Eckardt KU, Amann K, Kuro OM, Pasch A, Pieske B, Alesutan I. Signaling pathways involved in vascular smooth muscle cell calcification during hyperphosphatemia. *Cell Mol Life Sci* 2019;**76**:2077-2091.
11. Takemura A, Iijima K, Ota H, Son BK, Ito Y, Ogawa S, Eto M, Akishita M, Ouchi Y. Sirtuin 1 retards hyperphosphatemia-induced calcification of vascular smooth muscle cells. *Arterioscler Thromb Vasc Biol* 2011;**31**:2054-2062.
12. Nakano-Kurimoto R, Ikeda K, Uraoka M, Nakagawa Y, Yutaka K, Koide M, Takahashi T, Matoba S, Yamada H, Okigaki M, Matsubara H. Replicative senescence of vascular smooth muscle cells enhances the calcification through initiating the osteoblastic transition. *Am J Physiol Heart Circ Physiol* 2009;**297**:H1673-1684.
13. Yamada S, Tatsumoto N, Tokumoto M, Noguchi H, Ooboshi H, Kitazono T, Tsuruya K. Phosphate binders prevent phosphate-induced cellular senescence of vascular smooth muscle cells and vascular calcification in a modified, adenine-based uremic rat model. *Calcif Tissue Int* 2015;**96**:347-358.
14. Salazar G. NADPH Oxidases and Mitochondria in Vascular Senescence. *Int J Mol Sci* 2018;**19**.
15. Balogh E, Toth A, Mehes G, Trencsenyi G, Paragh G, Jeney V. Hypoxia Triggers Osteochondrogenic Differentiation of Vascular Smooth Muscle Cells in an HIF-1 (Hypoxia-Inducible Factor 1)-Dependent and Reactive Oxygen Species-Dependent Manner. *Arterioscler Thromb Vasc Biol* 2019;**39**:1088-1099.
16. Minol JP, Reinsch I, Luik M, Leferink A, Barth M, Assmann A, Lichtenberg A, Akhyari P. Focal induction of ROS-release to trigger local vascular degeneration. *PLoS One* 2017;**12**:e0179342.
17. Toth A, Balogh E, Jeney V. Regulation of Vascular Calcification by Reactive Oxygen Species. *Antioxidants (Basel)* 2020;**9**.
18. Kim S, Benguria A, Lai CY, Jazwinski SM. Modulation of life-span by histone deacetylase genes in Saccharomyces cerevisiae. *Mol Biol Cell* 1999;**10**:3125-3136.
19. Houtkooper RH, Pirinen E, Auwerx J. Sirtuins as regulators of metabolism and healthspan. *Nat Rev Mol Cell Biol* 2012;**13**:225-238.
20. Ford E, Voit R, Liszt G, Magin C, Grummt I, Guarente L. Mammalian Sir2 homolog SIRT7 is an activator of RNA polymerase I transcription. *Genes Dev* 2006;**20**:1075-1080.
21. Ashraf N, Zino S, Macintyre A, Kingsmore D, Payne AP, George WD, Shiels PG. Altered sirtuin expression is associated with node-positive breast cancer. *Br J Cancer* 2006;**95**:1056-1061.
22. Kim JK, Noh JH, Jung KH, Eun JW, Bae HJ, Kim MG, Chang YG, Shen Q, Park WS, Lee JY, Borlak J, Nam SW. Sirtuin7 oncogenic potential in human hepatocellular carcinoma and its regulation by the tumor suppressors MiR-125a-5p and MiR-125b. *Hepatology* 2013;**57**:1055-1067.
23. Barber MF, Michishita-Kioi E, Xi Y, Tasselli L, Kioi M, Moqtaderi Z, Tennen RI, Paredes S, Young NL, Chen K, Struhl K, Garcia BA, Gozani O, Li W, Chua KF. SIRT7 links H3K18 deacetylation to maintenance of oncogenic transformation. *Nature* 2012;**487**:114-118.
24. Araki S, Izumiya Y, Rokutanda T, Ianni A, Hanatani S, Kimura Y, Onoue Y, Senokuchi T, Yoshizawa T, Yasuda O, Koitabashi N, Kurabayashi M, Braun T, Bober E, Yamagata K, Ogawa H. Sirt7 Contributes to Myocardial Tissue Repair by Maintaining Transforming Growth Factor-beta Signaling Pathway. *Circulation* 2015;**132**:1081-1093.
25. Vakhrusheva O, Smolka C, Gajawada P, Kostin S, Boettger T, Kubin T, Braun T, Bober E. Sirt7

increases stress resistance of cardiomyocytes and prevents apoptosis and inflammatory cardiomyopathy in mice. *Circ Res* 2008;**102**:703-710.
26. Yamamura S, Izumiya Y, Araki S, Nakamura T, Kimura Y, Hanatani S, Yamada T, Ishida T, Yamamoto M, Onoue Y, Arima Y, Yamamoto E, Sunagawa Y, Yoshizawa T, Nakagata N, Bober E, Braun T, Sakamoto K, Kaikita K, Morimoto T, Yamagata K, Tsujita K. Cardiomyocyte Sirt (Sirtuin) 7 Ameliorates Stress-Induced Cardiac Hypertrophy by Interacting With and Deacetylating GATA4. *Hypertension* 2020;**75**:98-108.
27. Zheng J, Chen K, Wang H, Chen Z, Xi Y, Yin H, Lai K, Liu Y. SIRT7 Regulates the Vascular Smooth Muscle Cells Proliferation and Migration via Wnt/beta-Catenin Signaling Pathway. *Biomed Res Int* 2018;**2018**:4769596.
28. Osako MK, Nakagami H, Koibuchi N, Shimizu H, Nakagami F, Koriyama H, Shimamura M, Miyake T, Rakugi H, Morishita R. Estrogen inhibits vascular calcification via vascular RANKL system: common mechanism of osteoporosis and vascular calcification. *Circ Res* 2010;**107**:466-475.
29. He P, Yu H, Jiang L, Chen Z, Wang S, Macrae VE, Fu X, Zhu D. Hdac9 inhibits medial artery calcification through down-regulation of Osterix. *Vascul Pharmacol* 2020;**132**:106775.
30. Li W, Feng W, Su X, Luo D, Li Z, Zhou Y, Zhu Y, Zhang M, Chen J, Liu B, Huang H. SIRT6 protects vascular smooth muscle cells from osteogenic transdifferentiation via Runx2 in chronic kidney disease. *J Clin Invest* 2022;**132**.
31. Wang S, Li L, Liang Q, Ye Y, Lan Z, Dong Q, Chen A, Fu M, Li Y, Liu X, Ou JS, Lu L, Yan J. Deletion of SIRT6 in vascular smooth muscle cells facilitates vascular calcification via suppression of DNA damage repair. *J Mol Cell Cardiol* 2022;**173**:154-168.
32. Yoshizawa T, Sato Y, Sobuz SU, Mizumoto T, Tsuyama T, Karim MF, Miyata K, Tasaki M, Yamazaki M, Kariba Y, Araki N, Araki E, Kajimura S, Oike Y, Braun T, Bober E, Auwerx J, Yamagata K. SIRT7 suppresses energy expenditure and thermogenesis by regulating brown adipose tissue functions in mice. *Nat Commun* 2022;**13**:7439.
33. Kim JH, Kim D, Cho SJ, Jung KY, Kim JH, Lee JM, Jung HJ, Kim KR. Identification of a novel SIRT7 inhibitor as anticancer drug candidate. *Biochem Biophys Res Commun* 2019;**508**:451-457.
34. He F, Ru X, Wen T. NRF2, a Transcription Factor for Stress Response and Beyond. *Int J Mol Sci* 2020;**21**.
35. Li R, Jia Z, Zhu H. Regulation of Nrf2 Signaling. *React Oxyg Species (Apex)* 2019;**8**:312-322.
36. Kageyama S, Gudmundsson SR, Sou YS, Ichimura Y, Tamura N, Kazuno S, Ueno T, Miura Y, Noshiro D, Abe M, Mizushima T, Miura N, Okuda S, Motohashi H, Lee JA, Sakimura K, Ohe T, Noda NN, Waguri S, Eskelinen EL, Komatsu M. p62/SQSTM1-droplet serves as a platform for autophagosome formation and anti-oxidative stress response. *Nat Commun* 2021;**12**:16.
37. Touyz RM, Briones AM. Reactive oxygen species and vascular biology: implications in human hypertension. *Hypertens Res* 2011;**34**:5-14.
38. Roger L, Tomas F, Gire V. Mechanisms and Regulation of Cellular Senescence. *Int J Mol Sci* 2021;**22**.
39. Vigili de Kreutzenberg S, Giannella A, Ceolotto G, Faggin E, Cappellari R, Mazzucato M, Fraccaro C, Tarantini G, Avogaro A, Fadini GP. A miR-125/Sirtuin-7 pathway drives the pro-calcific potential of myeloid cells in diabetic vascular disease. *Diabetologia* 2022;**65**:1555-1568.
40. Li XT, Song JW, Zhang ZZ, Zhang MW, Liang LR, Miao R, Liu Y, Chen YH, Liu XY, Zhong JC. Sirtuin 7 mitigates renal ferroptosis, fibrosis and injury in hypertensive mice by facilitating the KLF15/Nrf2 signaling. *Free Radic Biol Med* 2022;**193**:459-473.
41. Chen EEM, Zhang W, Ye CCY, Gao X, Jiang LLJ, Zhao TTF, Pan ZZJ, Xue DDT. Knockdown of SIRT7 enhances the osteogenic differentiation of human bone marrow mesenchymal stem cells partly via activation of the Wnt/beta-catenin signaling pathway. *Cell Death Dis* 2017;**8**:e3042.
42. Fukuda M, Yoshizawa T, Karim MF, Sobuz SU, Korogi W, Kobayasi D, Okanishi H, Tasaki M, Ono K, Sawa T, Sato Y, Chirifu M, Masuda T, Nakamura T, Tanoue H, Nakashima K, Kobashigawa Y, Morioka H, Bober E, Ohtsuki S, Yamagata Y, Ando Y, Oike Y, Araki N, Takeda S, Mizuta H, Yamagata K. SIRT7 has a critical role in bone formation by regulating lysine acylation of SP7/Osterix. *Nat Commun* 2018;**9**:2833.
43. Huang M, Zheng L, Xu H, Tang D, Lin L, Zhang J, Li C, Wang W, Yuan Q, Tao L, Ye Z. Oxidative stress contributes to vascular calcification in patients with chronic kidney disease. *J Mol Cell Cardiol* 2020;**138**:256-268.
44. Cui L, Zhou Q, Zheng X, Sun B, Zhao S. Mitoquinone attenuates vascular calcification by suppressing

oxidative stress and reducing apoptosis of vascular smooth muscle cells via the Keap1/Nrf2 pathway. *Free Radic Biol Med* 2020;**161**:23-31.
45. Gao M, Li X, He Y, Han L, Qiu D, Ling L, Liu H, Liu J, Gu L. SIRT7 functions in redox homeostasis and cytoskeletal organization during oocyte maturation. *FASEB J* 2018:fj201800078RR.
46. Qiao Y. Reactive Oxygen Species in Cardiovascular Calcification: Role of Medicinal Plants. *Front Pharmacol* 2022;**13**:858160.
47. Forstermann U, Xia N, Li H. Roles of Vascular Oxidative Stress and Nitric Oxide in the Pathogenesis of Atherosclerosis. *Circ Res* 2017;**120**:713-735.
48. Shanahan CM. Mechanisms of vascular calcification in CKD-evidence for premature ageing? *Nat Rev Nephrol* 2013;**9**:661-670.
49. Li X, Liu A, Xie C, Chen Y, Zeng K, Xie C, Zhang Z, Luo P, Huang H. The transcription factor GATA6 accelerates vascular smooth muscle cell senescence-related arterial calcification by counteracting the role of anti-aging factor SIRT6 and impeding DNA damage repair. *Kidney Int* 2024;**105**:115-131.
50. Rodriguez S, Bermudez LG, Gonzalez D, Bernal C, Canas A, Morales-Ruiz T, Henriquez B, Rojas A. Transcriptional regulation of CDKN2A/p16 by sirtuin 7 in senescence. *Mol Med Rep* 2022;**26**.
51. Grootaert MO, da Costa Martins PA, Bitsch N, Pintelon I, De Meyer GR, Martinet W, Schrijvers DM. Defective autophagy in vascular smooth muscle cells accelerates senescence and promotes neointima formation and atherogenesis. *Autophagy* 2015;**11**:2014-2032.
52. Fang J, Ianni A, Smolka C, Vakhrusheva O, Nolte H, Kruger M, Wietelmann A, Simonet NG, Adrian-Segarra JM, Vaquero A, Braun T, Bober E. Sirt7 promotes adipogenesis in the mouse by inhibiting autocatalytic activation of Sirt1. *Proc Natl Acad Sci U S A* 2017;**114**:E8352-E8361.
53. Bartoli-Leonard F, Wilkinson FL, Schiro A, Inglott FS, Alexander MY, Weston R. Suppression of SIRT1 in Diabetic Conditions Induces Osteogenic Differentiation of Human Vascular Smooth Muscle Cells via RUNX2 Signalling. *Sci Rep* 2019;**9**:878.
54. Bartoli-Leonard F, Wilkinson FL, Schiro A, Serracino Inglott F, Alexander MY, Weston R. Loss of SIRT1 in diabetes accelerates DNA damage-induced vascular calcification. *Cardiovasc Res* 2021;**117**:836-849.

Figure legends

Figure 1. Reduced expression of *Sirt7* in mouse calcified arteries. (A) Representative images of alizarin red staining of the whole aortas from mice with control and overloaded vD_3, n=2. **(B)** Representative images of alizarin red staining of the aortic sections from mice with control and overloaded vD_3, scale bar=100μm. **(C)** Calcium quantification assay of the aortas from mice with control and overloaded vD_3 normalized to dry aortic weight, n=3. **(D)** RT-qPCR for mRNA expression of the osteogenic genes including *Runx2*, *Alpl* and *Opn*, and the Sirtuin family members including *Sirt1* to *Sirt7*, n=7-8. **(E)** Western blotting and semi-quantitative analysis of SIRT7 protein expression in control and calcified mouse arteries, n=6. Data are presented as mean ± SD, and statistical significance was analyzed by a two-tailed unpaired Student's t-test. *p < 0.05, **p < 0.01, ***p < 0.001 compared to control.

Figure 2. *Sirt7* inhibits vascular calcification *in vitro* and *in vivo*. (A) Representative images of alizarin red staining of VSMCs with control and depleted *Sirt7* expression. **(B)** Calcium quantification assay of VSMCs with control and depleted *Sirt7* expression, n=4. **(C)** Representative images of alizarin red staining of VSMCs with control and overexpression of wild type *Sirt7* and a loss-of-function mutant $Sirt7^{H188Y}$. **(D)** Calcium quantification assay of VSMCs transduced with control, *Sirt7* and $Sirt7^{H188Y}$, n=5. **(E)** Representative images of alizarin red staining of the whole mouse aortas from control, vD_3 and vD_3+ the *Sirt7* inhibitor 97491. **(F)** Calcium quantification assay of the mouse aortas from control, vD_3 and vD_3+ the *Sirt7* inhibitor 97491, n=5. Data are presented as mean ± SD, and statistical significance was analyzed by a one-way ANOVA followed by Tukey's multiple comparisons test. ***p < 0.001 compared to control. $^{\#\#}p<0.01$, $^{\#\#\#}p<0.001$ compared to high Pi, ad-Sirt7 or vD_3.

Figure 3. Knockdown of *Sirt7* in VSMCs induces Nrf2-mediated oxidative stress response. (A) Volcano plot with green dots representing significantly down-regulated protein-coding genes (n=312) and red dots representing significantly up-regulated protein-coding genes (n=229) in VSMCs with depleted *Sirt7*

expression. **(B)** Hierarchical clustering heatmap of 541 protein-coding genes differentially expressed in VSMCs with depleted *Sirt7* expression (The FDR < 0.01 & Fold Change ≥2), n=3. **(C)** The top 15 significantly up-regulated genes are listed in VSMCs with knockdown of *Sirt7*. **(D)** Top 11 up-regulated genes and 9 down-regulated genes identified by RNA-Seq were validated using RT-qPCR, n=4. **(E)** Correlation between RNA-Seq and RT-qPCR. Comparison of fold change of 20 genes obtained by RNA-Seq and RT-qPCR. **(F)** IPA pathway analysis of the differentially expressed genes in *Sirt7* depleted VSMCs identified by RNA-seq. **(G)** Immunofluorescence staining for the nucleus translocation of Nrf2 in control and *Sirt7* knockdown VSMCs, scale bar=25μm. **(H)** RNA-seq data for the mRNA expression of the Nrf2 key regulator *Keap1* and *p62*, n=3. **(I)** Western blotting for p62 protein expression in control and *Sirt7* depleted VSMCs. Data are presented as mean ± SD, and statistical significance was analyzed by a two-tailed unpaired Student's t-test. ***p < 0.001 compared to siScramble.

Figure 4. ROS mediates *Sirt7* knockdown-induced VSMC *in vitro* calcification. (A) Representative images of DCFHDA staining of intracellular ROS in VSMCs with control and depleted *Sirt7*, scale bar=100μm. **(B)** Semi-quantitative analysis of DCFHDA staining of intracellular ROS in VSMCs with control and depleted *Sirt7*, n=3. *p < 0.05 compared to siScramble + Normal Pi, $^{\#}$p < 0.05 compared to siScramble + High Pi. **(C)** MitoSox staining of mitochondrial ROS in VSMCs, scale bar=25μm. **(D)** RNA-seq data for mRNA expression *Xdh* and *Nox4* in control and *Sirt7* knockdown VSMCs, n=3. *p < 0.05 compared to siScramble. **(E)** Western blotting results for XDH protein expression in control and *Sirt7* depleted VSMCs. **(F)** Calcium quantitative assay in VSMCs treated as indicated**,** n=5. ***p < 0.001 compared to siScramble + High Pi, $^{\#}$p < 0.05 compared to si*Sirt7* + High Pi. Data are presented as mean ± SD, and statistical significance was analyzed by a one-way ANOVA followed by Tukey's multiple comparisons test.

Figure 5. Knockdown of *Sirt7* delays cell cycle progression and promotes cellular senescence in VSMCs. (A&B) FACs analysis of cell cycle phase in VSMCs transfected with siScramble and si*Sirt7*, n=3. *p < 0.05 compared to siScramble + Normal Pi, $^{\#}$p < 0.05 compared to siScramble+ High Pi. **(C)** Western blotting of the cell cycle regulator p-RB, RB and cyclin D1 protein expression. **(D&E)** SA-β-Gal staining and semi-quantitative assay of cellular senescence in VSMCs with control and depleted *Sirt7* expression, n=3. **p < 0.01 compared to siScramble + Normal Pi, $^{\#\#\#}$p < 0.001 compared to siScramble + High Pi. **(F)** Western blotting for cell senescence marker p16 and p21 protein expression. Data are presented as mean ± SD, and statistical significance was analyzed by a two-tailed unpaired Student's t-test.

Figures

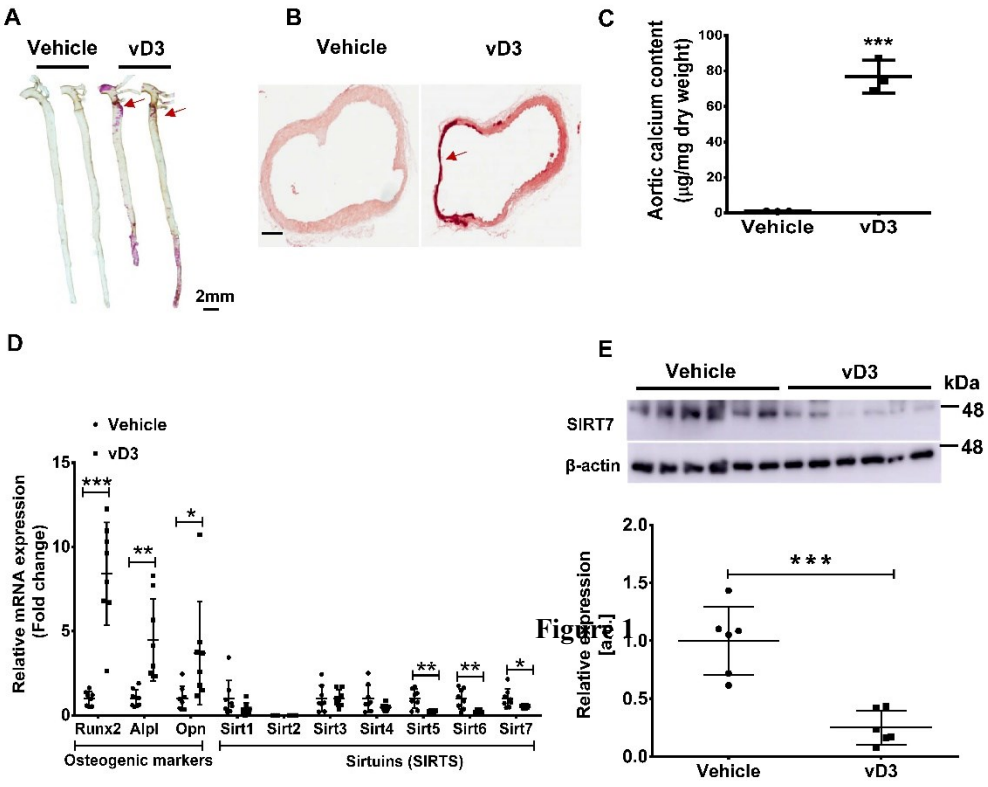

Figure 1

Figure 1

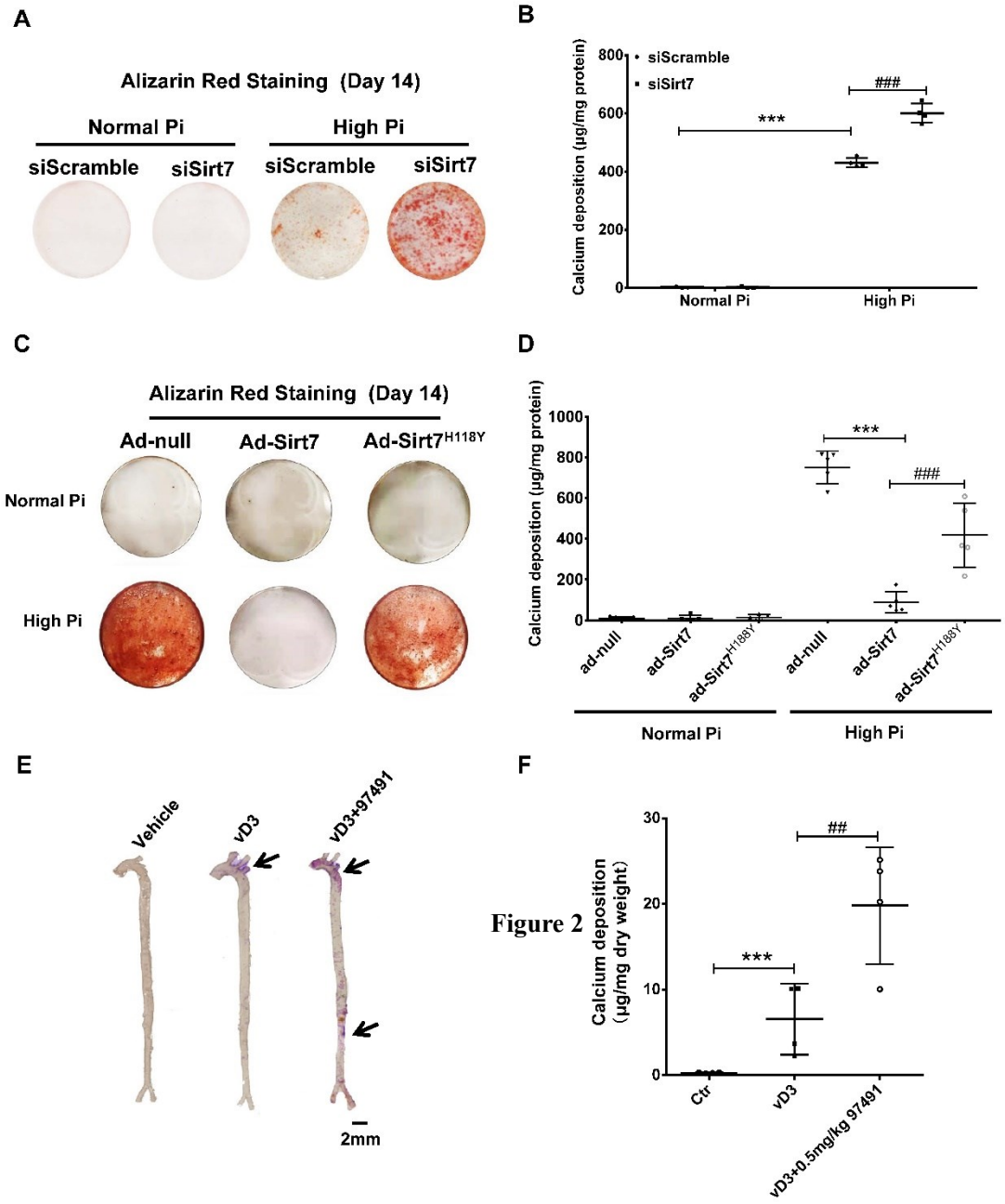

Figure 2

Figure 2

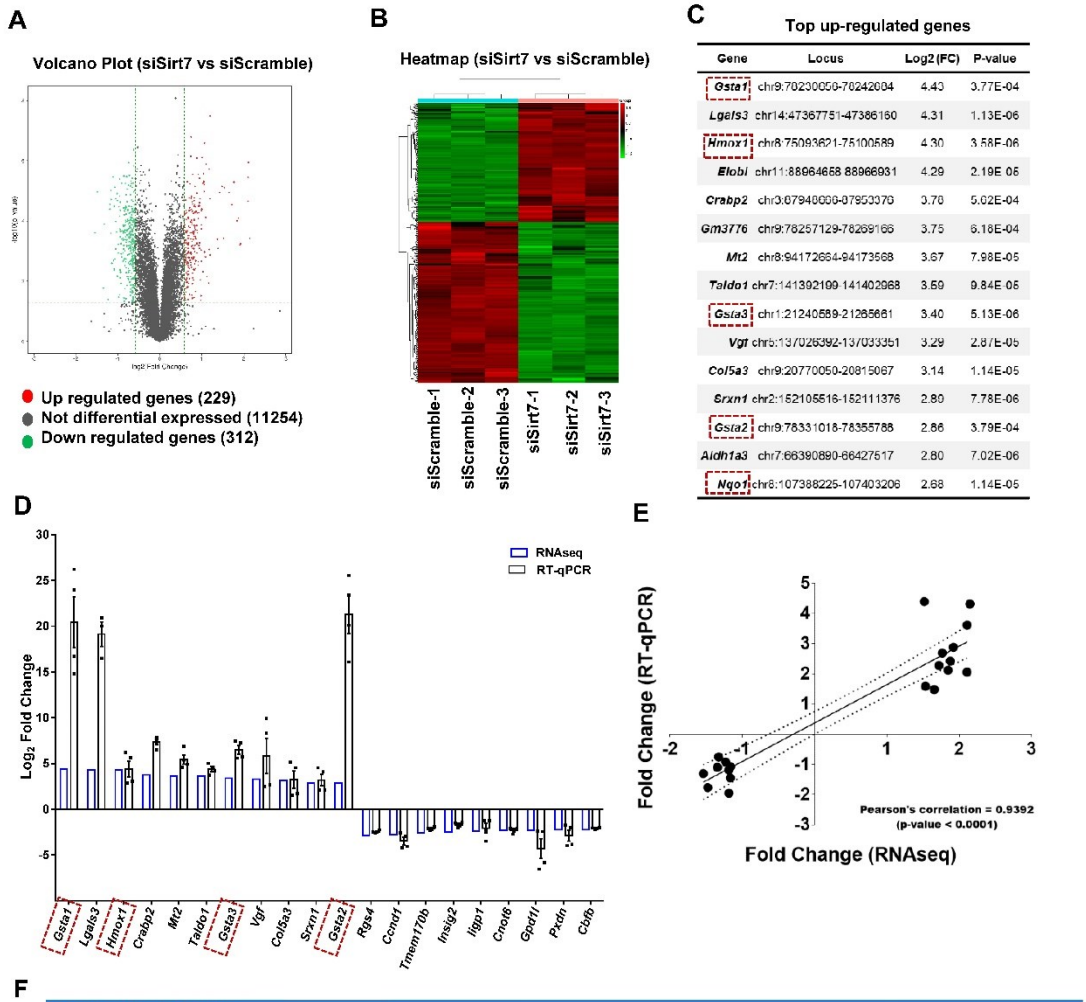
A
Volcano Plot (siSirt7 vs siScramble)
Up regulated genes (229)
Not differential expressed (11254)
Down regulated genes (312)
B
Heatmap (siSirt7 vs siScramble)
siScramble-1
siScramble-2
siScramble-3
siSirt7-1
siSirt7-2
siSirt7-3
C
Top up-regulated genes
Gene Locus Log2 (FC) P-value
Gsta1 chr9:70230050-70242004 4.43 3.77E-04
Lgals3 chr14:47367751-47386160 4.31 1.13E-06
Hmox1 chr8:75093621-75100589 4.30 3.58E-06
Elobl chr11:88964658-88966931 4.29 2.19E-05
Crabp2 chr3:07940000-07950370 3.70 5.02E-04
Gm3776 chr9:76257129-76269166 3.75 6.18E-04
Mt2 chr8:94172664-94173568 3.67 7.98E-05
Taldo1 chr7:141392109-141402968 3.59 9.84E-05
Gsta3 chr1:21240589-21265661 3.40 5.13E-06
Vgf chr5:137026392-137033351 3.29 2.87E-05
Col5a3 chr9:20770050-20815067 3.14 1.14E-05
Srxn1 chr2:152105516-152111376 2.80 7.78E-06
Gsta2 chr9:78331018-78355788 2.66 3.79E-04
Aldh1a3 chr7:66390890-66427517 2.60 7.02E-06
Nqo1 chr8:107388225-107403206 2.58 1.14E-05
D
RNAseq
RT-qPCR
Log2 Fold Change
Gsta1 Lgals3 Hmox1 Crabp2 Mt2 Taldo1 Gsta3 Vgf Col5a3 Srxn1 Gsta2 Rgs4 Ccnd1 Tmem170b Insig2 Ifigp1 Cnot6 Gpd1l Pxdn C5fb
E
Fold Change (RT-qPCR)
Fold Change (RNAseq)
Pearson's correlation = 0.9392
(p-value < 0.0001)
F
Top Canonical Pathways
Name p-value Overlap
Mitotic Roles of Polo-Like Kinase 2.95E-07 16.7 % 11/66
Cell Cycle: G2/M DNA Damage Checkpoint Regulation 1.53E-06 18.4 % 9/49
NRF2-mediated Oxidative Stress Response 1.92E-05 7.9 % 16/202
Aryl Hydrocarbon Receptor Signaling 1.13E-04 8.5 % 12/142
Hepatic Fibrosis / Hepatic Stellate Cell Activation 7.0 % 13/186
G
siScramble
siSirt7
NRF2/DAPI
H
siScramble
siSirt7
***
RNA-seq (FPKM)
Keap1
Sqstm1 (p62)
I
Normal Pi
High Pi
siScramble
siSirt7
siScramble
siSirt7
kDa
p62
SIRT7
β-actin
63
48
48

Figure 3

Figure 3

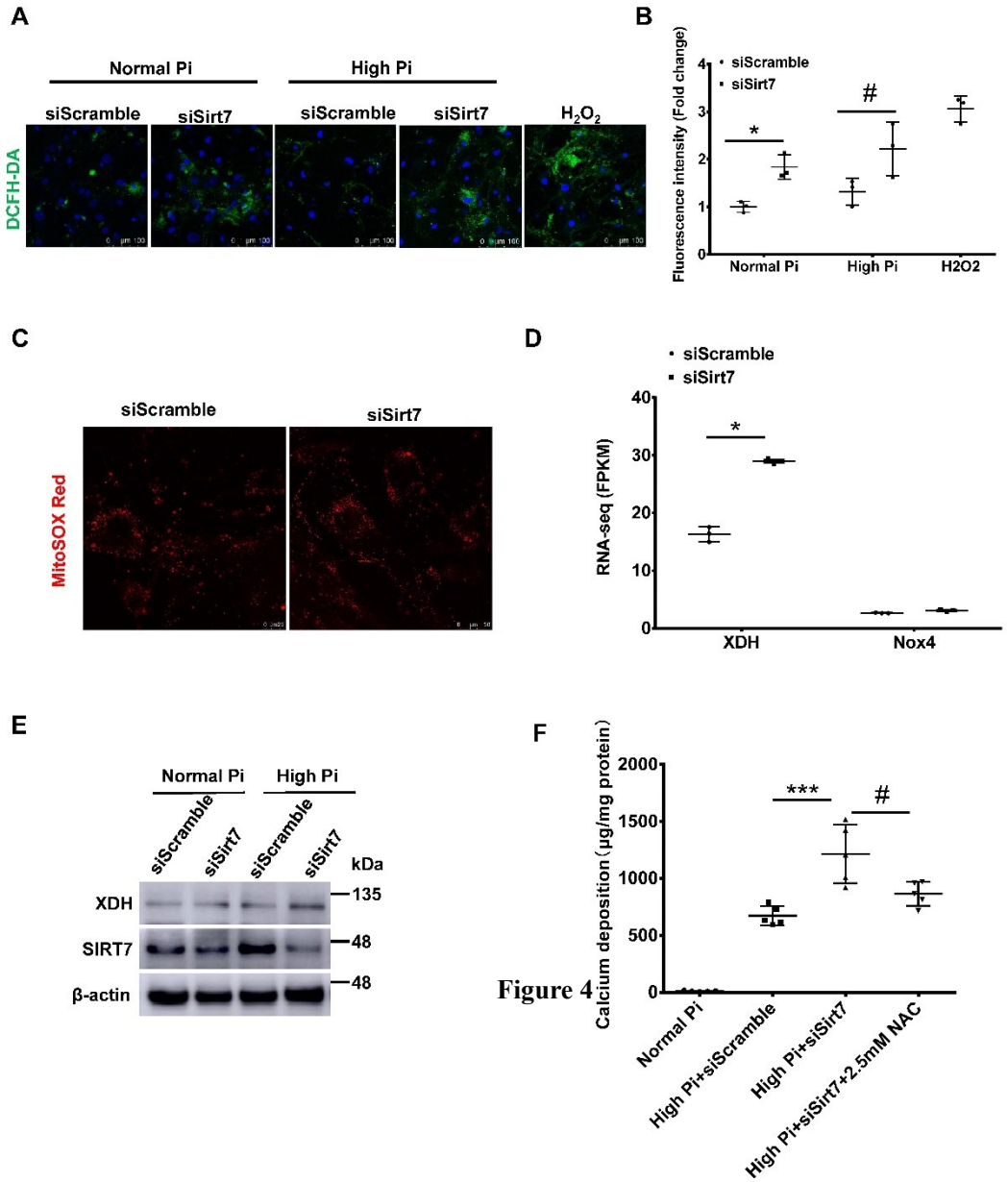

Figure 4

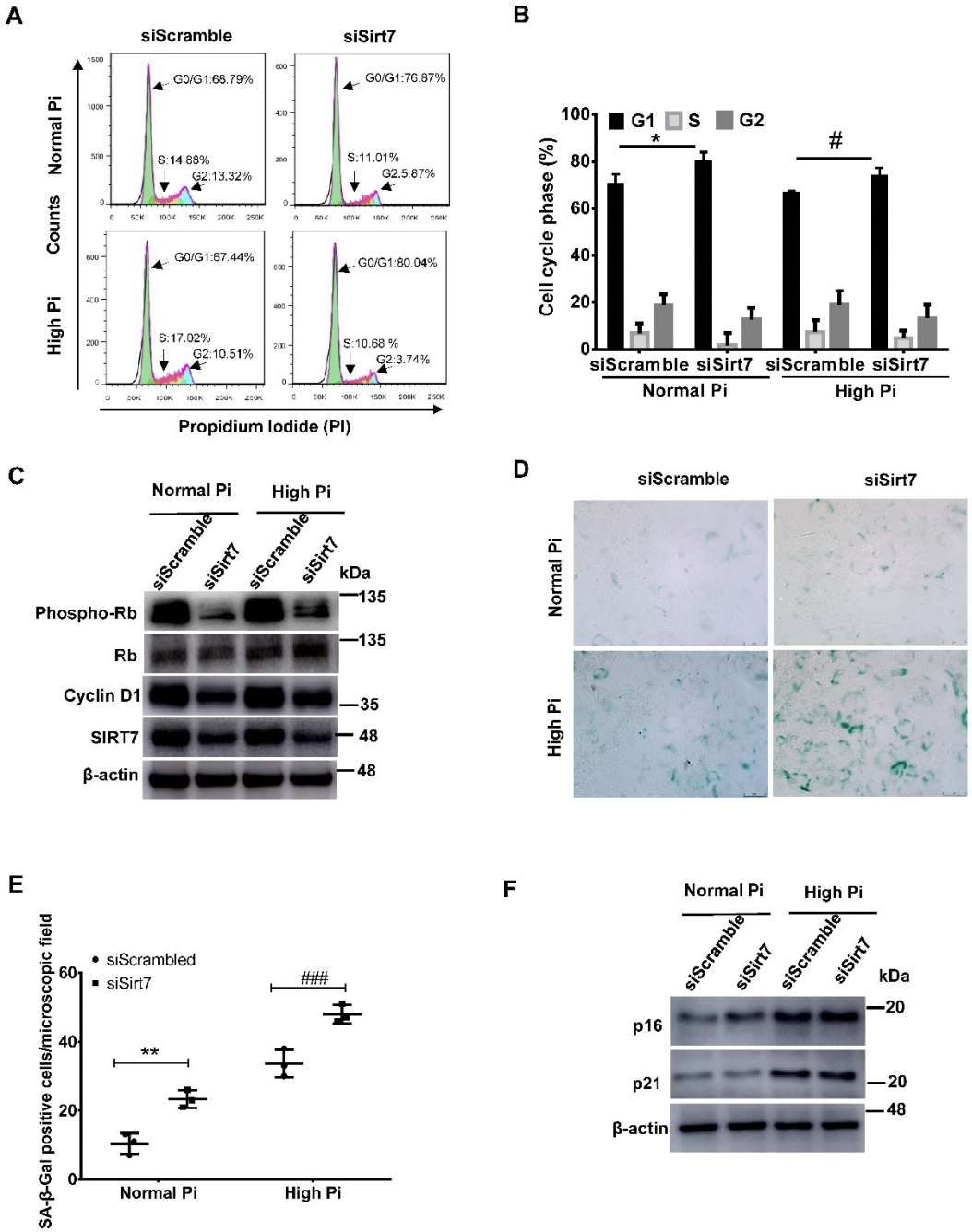
A
siScramble
siSirt7
Normal Pi
High Pi
Counts
G0/G1:68.79%
S:14.88%
G2:13.32%
G0/G1:76.87%
S:11.01%
G2:5.87%
G0/G1:67.44%
S:17.02%
G2:10.51%
G0/G1:80.04%
S:10.68 %
G2:3.74%
Propidium Iodide (PI)
B
G1
S
G2
Cell cycle phase (%)
siScramble
siSirt7
Normal Pi
High Pi
C
Phospho-Rb
Rb
Cyclin D1
SIRT7
β-actin
kDa
135
35
48
D
E
siScrambled
siSirt7
SA-β-Gal positive cells/microscopic field
F
p16
p21
β-actin
20
48

Figure 5

Supplementary Materials

Sirt7 protects against vascular calcification via modulation of reactive oxygen species and senescence of vascular smooth muscle cells

Hongjiao Yu[1,2#], Yuchen Xie[3#], Lan Lan[4#], Siyu Ma[2], Simon Wing Fai Mok[5], Io Nam Wong[5], Yueheng Wang[3], Guoli Zhong[3], Liang Yuan[3], Huan Zhao[3], Xiao Hu[6], Vicky E Macrae[7], Shengping He[8*], Guojun Chen[6*], Dongxing Zhu[3*]

9. Department of Hepatobiliary and Pancreatic Surgery, The Second Affiliated Hospital, Guangzhou Medical University, Guangzhou, 510260, China
10. GMU-GIBH Joint School of Life Sciences, The Guangdong-Hong Kong-Macao Joint Laboratory for Cell Fate Regulation and Diseases, Guangzhou Medical University.
11. Guangzhou Institute of Cardiovascular Disease, Guangdong Key Laboratory of Vascular Diseases, State Key Laboratory of Respiratory Disease, The Second Affiliated Hospital, School of Basic Medical Sciences, Guangzhou Medical University, Guangzhou, Guangdong, 510260, China.
12. Department of Anesthesiology, The First Affiliated Hospital of Guangzhou Medical University, Guangzhou, China.
13. Faculty of Medicine, Macau University of Science and Technology, Taipa, Macau, China.
14. Department of Cardiology, Guangdong Provincial Key Laboratory of Cardiac Function and Microcirculation, State Key Laboratory of Organ Failure Research, Nanfang Hospital, Southern Medical University, Guangzhou, China
15. Functional Genetics and Development, The Royal (Dick) School of Veterinary Studies and The Roslin Institute, University of Edinburgh, Midlothian, UK.
16. Department of Cardiovascular Surgery, Nanfang Hospital, Southern Medical University, 1838 North Guangzhou Avenue, Guangzhou, Guangdong 510515, China.

This word file includes:

- **Figures S1-S6**
- **Tables S1-S4**

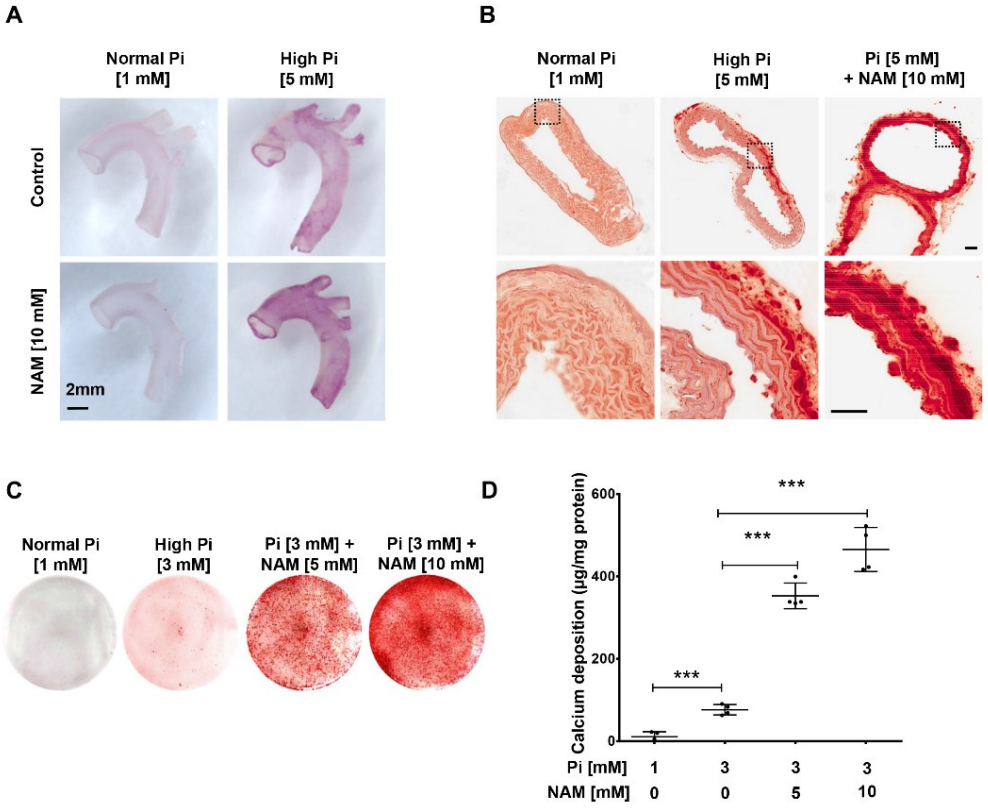

Figure S1. The pan inhibitor of Sirtuins NAM promotes high Pi-induced mouse aortic ring and VSMC calcification *in vitro*. (A) Representative images of alizarin red staining of the whole mouse aortic rings under normal and high Pi in the absence or presence of NAM. **(B)** Representative images of alizarin red staining of the sections of aortic rings under normal and high Pi in the absence or presence of NAM. **(C)** Representative images of alizarin red staining of VSMC under normal and high Pi with or without NAM. **(D)** Calcium quantitative assay for calcium deposition in VSMCs treated as indicated, n=4. Data are presented as mean ± SD, and statistical significance was analyzed by a one-way ANOVA followed by Tukey's multiple comparisons test. ***p < 0.001.

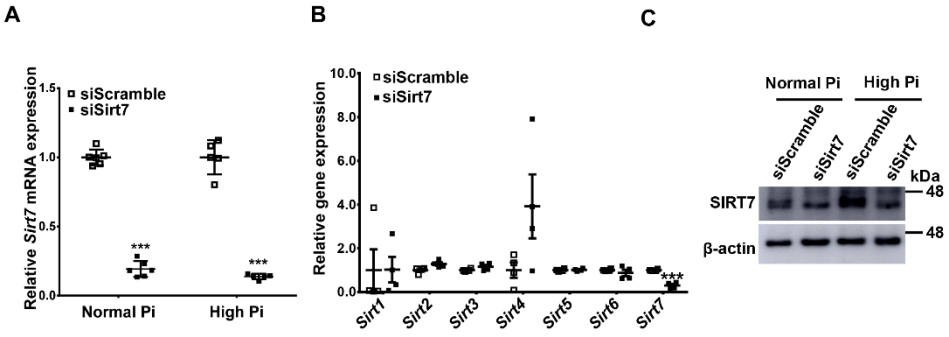

Figure S2. The validation of *Sirt7* knockdown efficiency and specificity in VSMCs. (A) RT-qPCR for *Sirt7* expression in VSMCs transfected with siScramble and si*Sirt7*, n=6. ***p < 0.001 compared to siScramble. **(B)** RT-qPCR for *Sirt1*-*Sirt7* expression in VSMCs transfected with siScamble and si*Sirt7*, n=4. ***p < 0.001 compared to siScramble. **(C)** Western blotting for SIRT7 protein expression in VSMCs transfected with siScamble and si*Sirt7*. Data are presented as mean ± SD, and statistical significance was analyzed by a two-tailed unpaired Student's t-test or one-way ANOVA followed by Tukey's multiple comparisons test.

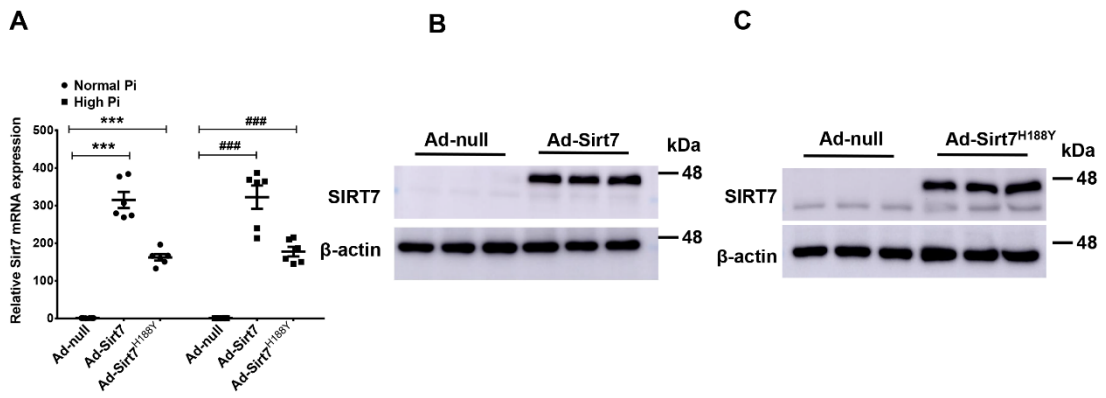

Figure S3. The validation of *Sirt7* overexpression efficiency in VSMCs transduced with ad-*Sirt7* and ad-*Sirt7*^{H188Y}. (A) RT-qPCR for *Sirt7* expression in VSMCs treated as indicated, n=6. ***p < 0.001 compared to Ad-null + Normal Pi, ###p < 0.001 compared to Ad-null + High Pi. **(B&C)** Western blotting for SIRT7 protein expression in VSMCs treated as indicated, n=3. Data are presented as mean ± SD, and statistical significance was analyzed by a one-way ANOVA followed by Tukey's multiple comparisons test.

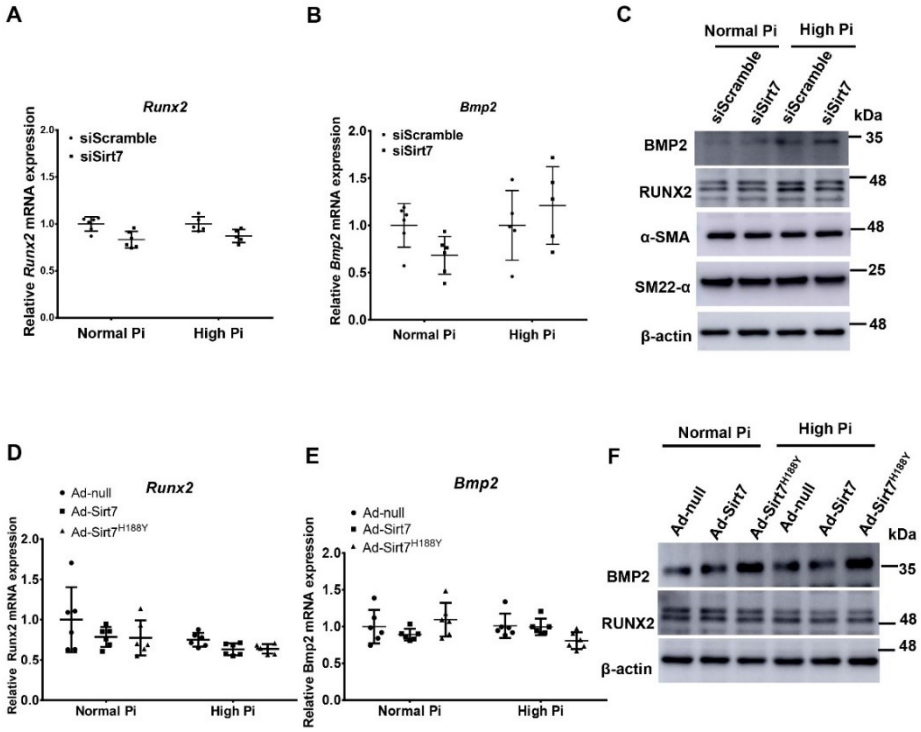

Figure S4. *Sirt7* does not alter the osteogenic and contractile gene expression in VSMCs. (A&B) RT-qPCR for *Runx2* and *Bmp2* mRNA expression in VSMCs with control or depleted *Sirt7*, n=6. **(C)** Western blotting for RUNX2, BMP2, α-SMA and SM22-α protein expression. **(D&E)** RT-qPCR for *Runx2* and *Bmp2* mRNA expression in VSMCs overexpressing *Sirt7* and *Sirt7*^{H188Y}, n=6. **(D)** Western blotting for RUNX2 and BMP2 protein expression in VSMCs with overexpression of *Sirt7* and *Sirt7*^{H188Y}. Data are presented as mean ± SD, and statistical significance was analyzed by a one-way ANOVA followed by Tukey's multiple comparisons test.

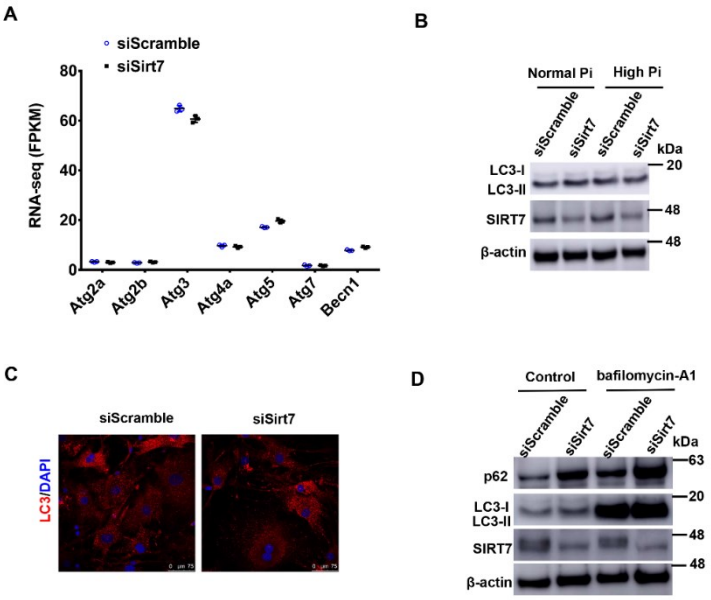

Figure S5. The regulation of *Sirt7* on p62 protein expression in VSMCs is independent of autophagy. **(A)** RNA-seq results of the key autophagy regulators in VSMCs with depleted *Sirt7* expression, n=3. **(B)** Western blotting for the autophagy maker LC3-I and LC3-II expression in control and *Sirt7* knockdown VSMCs. **(C)** Immunofluorescence staining of LC3 in VSMCs with control and depleted *Sirt7* expression. **(D)** Western blotting for p62 protein expression in VSMCs with control or silenced *Sirt7* expression in the absence or presence of Bafilnomycin-A1. Data are presented as mean ± SD, and statistical significance was analyzed by a two-tailed unpaired Student's t-test.

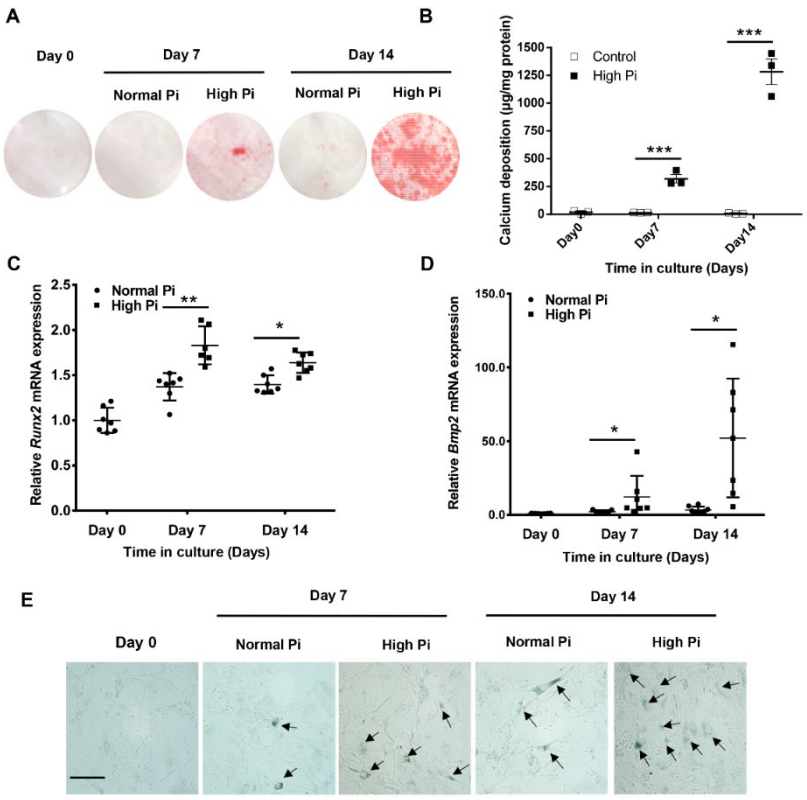

Figure S6. Cellular senescence is increased during high Pi-induced VSMC *in vitro* calcification. (A) Representative images of alizarin red staining. **(B)** Calcium quantitative assay of VSMCs, n=3. **(C)** RT-qPCR for *Runx2* and *Bmp2* mRNA expression in VSMCs, n=6. **(D)** SA-β-Gal staining for senescent VSMCs during the calcification process. Data are presented as mean ± SD, and statistical significance was analyzed by a one-way ANOVA followed by Tukey's multiple comparisons test. *p < 0.05, **p < 0.01, ***p < 0.001.

Table S1. The sequences of RT-qPCR primers used in this study

RT-qPCR primer sequences for target genes	
Genes of interest	**Primer sequences (5'-3')**
Gsta1	Forward: AAGCCCGTGCTTCACTACTTC Reverse: GGGCACTTGGTCAAACATCAAA
Lgals3	Forward: AGACAGCTTTTCGCTTAACGA Reverse: GGGTAGGCACTAGGAGGAGC
Hmox1	Forward: AAGCCGAGAATGCTGAGTTCA Reverse: GCCGTGTAGATATGGTACAAGGA
Crabp2	Forward: ATGCCTAACTTTTCTGGCAACT Reverse: GCACAGTGGTGGAGGTTTTGA
Mt2	Forward: GCCTGCAAATGCAAACAATGC Reverse : AGCTGCACTTGTCGGAAGC
Taldo1	Forward: GTAAAGCGCCAGAGGATGGAG Reverse: CTCTTGGTAGGCAGGCATCT
Gsta3	Forward: AAGAATGGAGCCTATCCGGTG Reverse: CCATCACTTCGTAACCTTGCC
Vgf	Forward: TGACACCGGCTGTCTCT Reverse: GGATCAGTAGAAGGAAGCAGAAG
Col5a3	Forward: CGGGGTACTCCTGGTCCTAC Reverse: GCATCCCTACTTCCCCCTTG
Srxn1	Forward: ACGGTGCACAACGTACCAAT Reverse: TCAGGGTCCGCCAGGAT
Gsta2	Forward: CACACTCCTCTGGAGCTGGAT Reverse: CCCGGGCATTGAAGTAGTGA
Aldh1a3	Forward: GGGTCACACTGGAGCTAGGA Reverse: CTGGCCTCTTCTTGGCGAA
Nqo1	Forward: AGGATGGGAGGTACTCGAATC Reverse: AGGCGTCCTTCCTTATATGCTA
Rgs4	Forward: GAGTGCAAAGGACATGAAACATC Reverse: TTTTCCAACGATTCAGCCCAT
Ccnd1	Forward: GCGTACCCTGACACCAATCTC Reverse: CTCCTCTTCGCACTTCTGCTC
Tmem170b	Forward： ACCTCACGGAGATGTGGTACT Reverse： GCTCCAGTTACAGAAGCCAGAA
Insig2	Forward：GGAGTCACCTCGGCCTAAAAA Reverse：CAAGTTCAACACTAATGCCAGGA
Iigp1	Forward： CAGGACATCCGCCTTAACTGT Reverse：AGGAAGTAAGTACCCATTAGCCA
Cnot6	Forward： CCTGACCCTCGGAGGATGTA Reverse：AAGTGAGTGAGTGACCACAAAG
Gpd1l	Forward： CCTCTGAAAGTGTGCATCGTG Reverse： GACGGTGGAGGAGAATTTCTG
Pxdn	Forward：ATTGACAGGCAAGCATTTAAGGG

	Reverse： CAGGGTCCAGCGTTTCTATCT
Cbfb	Forward：CCGCGAGTGCGAGATTAAGTA
	Reverse：GTTCTGGAAGCGTGTCTGG
SirT1	Forward：GCTGACGACTTCGACGACG
	Reverse：TCGGTCAACAGGAGGTTGTCT
SirT2	Forward： GCCTGGGTTCCCAAAAGGAG
	Reverse： GAGCGGAAGTCAGGGATACC
Sirt3	Forward： ATCCCGGACTTCAGATCCCC
	Reverse：CAACATGAAAAAGGGCTTGGG
Sirt4	Forward： CAAAGGCTGGAAATGAACT
	Reverse：TTGCCACCTCTAGGATTC
Sirt5	Forward：CTCCGGGCCGATTCATTTCC
	Reverse： GCGTTCGCAAAACACTTCCG
Sirt6	Forward：ATGTCGGTGAATTATGCAGCA
	Reverse： GCTGGAGGACTGCCACATTA
Sirt7	Forward：AGCATCACCCGTTTGCATGA
	Reverse： GGCAGTACGCTCAGTCACAT
Runx2	Forward：GACTGTGGTTACCGTCATGGC
	Reverse：ACTTGGTTTTTCATAACAGCGGA
Alpl	Forward：GTGACTACCACTCGGGTGAAC
	Reverse：CTCTGGTGGCATCTCGTTATC
Opn	Forward：AATGCTGTGTCCTCTGAA
	Reverse： TCGTCATCATCATCGTCAT

Table S2. The antibodies used in this study

Source of primary antibodies used in the present study

Antibodies	**Source**	**Catalogue No.**	**Application and dilution**
BMP2	Abcam, Rabbit	ab214821	Western blotting, 1:2000 in 5%BSA
RUNX2	Abcam, Rabbit	ab23981	Western blotting, 1:2000 in 5%BSA
SirT7	CST， Rabbit	5360	Western blotting, 1:2000 in 5%BSA
p16	Abcam， Rabbit	ab211542	Western blotting, 1:2000 in 5%BSA
p21	Abcam， Rabbit	ab109199	Western blotting, 1:2000 in 5%BSA
NRF2	Abcam， Rabbit	ab137550	Western blotting, 1:2000 in 5%BSA
β-actin	Santa， Mouse	sc81178	Western blotting, 1:2000 in 5%BSA

Table S3. The siRNA sequences for Sirt7

siRNA sequences targeting SirT7

Taget gene	Catalogue No.	Sequences (5'-3')
siSirT7-1	siB15513132543	GCAGCTTCTATCCCAGATT
siSirT7-2	siB15513132641	GCCCGGAGTTGACAAAGAA
siSirT7-3	siB15513132616	GCTCCATGGGAATATGTAT

Table S4. Blood serum parameters of control and vD_3 treated mice in the presence or absence of the Sirt7 inhibitor 97491

Data are expressed as mean ± SD (n=5-6). CREA, Creatinine.UA, Uric acid. BUN, Blood urea nitrogen.

Parameters	Control	vD_3	vD_3+0.5mg/kg 97491	P value (Control&vD_3)	P value (vD_3&vD_3+0.5mg/kg 97491)
Calcium (mmol/L)	2.34±0.43	4.07±0.78	4.25±0.75	0.0031	0.9608
Phosphorus (mmol/L)	1.75±0.16	2.10±0.53	2.02±0.51	0.3547	0.9482
CREA (μmol/L)	20.52±3.64	37.46±8.44	36.25±5.62	0.0008	0.9499
UA (μmol/L)	33.96±10.01	101.6±53.1	60.56±19.82	0.0103	0.1503
BUN (mg/dl)	19.95±2.09	41.27±21.15	53.76±16.44	0.0749	0.3683

Statistical analysis was performed using one-way ANOVA followed by Turkey's test.